Arabidopsis PIEZO regulates magnetic field-mediated root growth under blue light

Ziai Peng[a#], Wenjing Yang[b#], Man Dong[a#], Hanrui Bai[b,e], Yan Lei[a], Ninghui Pan[a], Yong Xie[a,c,d], Liwei Guo[a,c,d], Changning Liu[b]*, Yunlong Du[a,c,d]*

[a]College of Plant Protection, Yunnan Agricultural University, Kunming 650201, China.

[b]CAS Key Laboratory of Tropical Plant Resources and Sustainable Use, Yunnan Key Laboratory of Crop Wild Relatives Omics, State Key Laboratory of Plant Diversity and Specialty Crops, Xishuangbanna Tropical Botanical Garden, Chinese Academy of Sciences, Kunming 650223, China

[c]State Key Laboratory for Conservation and Utilization of Bio-Resources in Yunnan, Yunnan Agricultural University, Kunming 650201, China.

[d]Key Laboratory of Agro-Biodiversity and Pest Management of Education Ministry of China, Yunnan Agricultural University, Kunming 650201, China.

[e]College of Life Sciences, Division of Life Sciences and Medicine, University of Science and Technology of China, Hefei 230026, China

[#]These authors contributed equally to this work.

*Corresponding author: Yunlong Du, yunlongdu@aliyun.com; Changning Liu, liuchangning@xtbg.ac.cn;

Abstract:

The mechanosensitive protein PIEZO has a function in root growth. However, the mechanisms underlying the effects of *PIEZO* responses to magnetic field (MF) remain elusive. Here, we report that *Arabidopsis PIEZO* gene regulation of root growth was responsive to MF and blue light. Mutation of *PIEZO* results in a shorter root length under MF treatment and blue light. Moreover, expression of *PIEZO* in root tips was up-regulated by an unknown blue-light-induced signal, transferred from the leaves to the roots in the presence of a MF. Furthermore, *PIEZO* was able to regulate calcium ion efflux and disturb auxin transport under MF and blue light. Interestingly, the blue light receptors CRY1 and 2 were necessary both for MF perception and regulation of root growth. Transcriptome analysis of the *piezo-cl* mutant grown in a MF and under blue light revealed that the *PIEZO* involved in regulation of root growth is also involved in indirect or direct interactions with gibberellin 4 (GA4), ethylene, calcium ion-related genes, mechanosensors and microRNA. Moreover, the expression of *miR5648-5p* conferred MF sensitivity and showed a way that *PIEZO* could be negatively regulated in a MF and blue light. Our data reveal the mechanism of *PIEZO* responds to MF and blue light to regulate root growth, in which converges different pathways, involving phytohormones, mechanosensors, calcium ions and blue light, as key components.

One-Sentence Summary: PIEZO perceives magnetic fields and blue light to regulate *Arabidopsis* root growth

Introduction

Magnetic field (MF) is essential to organism survival. MF plays an important role in plant growth (Hafeez et al., 2023; Tapia-Belmonte et al., 2023; Saletnik et al., 2022; da Silva and Dobránszki, 2016), and can regulate plant root growth (González-Vidal et al., 2022; Vashisth and Joshi, 2017) associated with cryptochromes (CRY, a class of flavoproteins sensitive to blue light), the auxin signaling pathway (Jin et al., 2019; Xu et al., 2018; Xu et al., 2015), and calcium ion (Ca^{2+}) homeostasis (Narayana et al., 2018; Belyavskaya, 2004). In *Arabidopsis* seedlings grown in the International Space Station (where the galactic MF is 0.1-1 nT (Belyavskaya, 2004)), the expression levels of genes related to regulation of calcium content are changed compared with Earth-grown seedlings (Correll et al., 2013). Furthermore, the effect of MF on plant growth linked to the light response, including the blue light response, is associated with an increase in Ca^{2+} influx (Grinberg et al., 2022) and the CRY-dependent signaling pathways (Albaqami et al., 2020; Agliassa et al., 2018, Ahmad et al., 2007). Importantly, blue light-induced root growth is mediated by CRY (Canamero et al., 2006) and auxin transport is regulated by PIN-FORMED3 (PIN3) in *Arabidopsis* (Zhai et al., 2021; Zhang et al., 2013). The responses of shoot apical meristems (SAMs) to mechanical stress involve transient changes in cytoplasmic Ca^{2+} concentrations, which are necessary to establish PIN1 polarity (Li et al., 2019) and nuclear translocation of the photoreceptor phyB (Zhao et al., 2023). The role of the Ca^{2+} in the regulation of root development is associated with auxin (Wang et al., 2022; Chakraborty et al., 2021; Zhang et al., 2020; Leitão et al., 2019; Vanneste and Friml, 2013). Complexes of the Ca^{2+} signaling module CALMODULIN IQ-MOTIF CONTAINING PROTEIN (CaM-IQM) interact with auxin signaling repressors, in which the CaM6 interacts physically with IAA19, to regulate root development (Zhang et al., 2022). However, the relationship among MF, blue light, phytohormones (including auxin), and Ca^{2+} in the regulation of root growth remains unclear.

The PIEZO protein is an evolutionarily conserved mechanosensor in land plants (Ashraf, 2021). PIEZO is a component of mechanically activated cation channels (Coste et al., 2010) and can convert physico-mechanical stimuli into bioelectrical signals (Yang et al., 2022). The *Arabidopsis* PIEZO and its moss homologs localize to the tonoplast and regulate vacuole morphology (Radin et al., 2021). Moreover, *AtPIEZO* can act as a calcium channel during the perception of mechanical force to regulate root growth (Mousavi et al., 2021; Fang et al., 2021). Furthermore, the FER-PIF3-PIEZO circuitry is known to control penetration of primary roots

into compacted soil (Bello-Bello and Herrera-Estrella, 2024; Xu et al., 2024). The rice *PIEZO* gene contains several different *cis*-acting elements related to light and the phytohormones methyl jasmonate (MeJA) and GA (Hu et al., 2021). The function of *PIEZO* in the regulation of root growth is therefore connected to the presence of phytohormones (including auxin), and light. However, whether *PIEZO* is able to respond to a MF and blue light simultaneously to change Ca^{2+} homeostasis and auxin transport and thus regulate root growth remains unclear. In this study, we found that the *PIEZO* gene was able to perceive MF to regulate root growth dependent on the presence of blue light. Furthermore, *PIEZO* regulation of root growth occurred via a converged pathway involving the phytohormones auxin, GA and ethylene, calcium ions, mechanosensors and blue light in the presence of a MF. These results revealed an undiscovered mechanism by which *PIEZO* may regulate root growth through the perception of MF and blue light.

Results

The *Arabidopsis PIEZO* gene can respond to magnetic field direction in a blue light-dependent manner to affect root growth

To test whether the *PIEZO* gene responds to MF, we firstly assessed the effect on *PIEZO* regulation of root growth when subjected to a 500 mT MF and to red or blue light, where the direction of the magnetic field was perpendicular to the direction of gravity (Fig. 1A). When seedlings were grown under red light (Fig. 1B-G), compared with those seedlings not subjected to MF treatment (Fig. 1B, E), the primary root lengths of wild-type (WT) Col-0 (Fig. 1C-D) and *piezo-cl* mutant (Fig. 1F-G) seedlings subjected to a MF were significantly shorter (Fig. 1N) and showed a decreased root growth angle (Fig. 1P-Q). However, when the seedlings were grown under blue light (Fig. 1H-M), compared with the control not subjected to a MF (Fig. 1H, K), the primary root lengths of WT seedlings did not show any obvious change in the presence of a MF (Fig. 1O), but the root lengths of *piezo-cl* mutant seedlings were significantly shorter (Fig. 1O). The root growth angle did not show any obvious change in the WT, but increased in the *piezo-cl* mutant when seedlings were grown in a MF under blue light (Fig. 1R). Similarly, the primary root length and root growth angle of a T-DNA insertion mutant *piezo-T* grown under red or blue light and subjected to MF treatment showed the same phenotype as the *piezo-cl* mutant seedlings (Fig. 1A-R, S1).

When we checked the expression levels of *PIEZO* following different treatment times (15 min, 30 min, 72 hr and 144 hr), we found that the levels of *PIEZO* had increased in the WT seedlings grown under blue light in a 500 mT MF (Fig. 1S). When a transgenic *Arabidopsis* expressing *proPIEZO::GUS* was grown under blue light and with a 500 mT MF, the levels of the GUS gene also increased compared with the control without MF treatment (Fig. S2). This demonstrates that the *PIEZO* gene is able to perceive MF.

When seedlings overexpressing the *PIEZO* gene were grown under red or blue light in the presence of a MF (Fig. S3A-Y), compared with the control without MF treatment, the WT and *PIEZO*-overexpressing lines #4, #9 and #16 showed reduced root length (Fig. S3Z) and root growth angle (Fig. S3AB) under red light, however, the root length (Fig. S3AA) and root growth angle (Fig. S3AC) did not show significant differences in these lines when grown under blue light.

To detect the effects of different MF polarity and direction of gravity on *PIEZO* gene regulation of seedling root growth, WT and *piezo-cl* mutant seedlings were subjected to a 500mT MF, where the direction of the MF was either parallel (Fig. S4A) or anti-parallel (Fig. S4B) to the direction of gravity, under either red or blue light. Compared with the seedlings not subjected to MF treatment, the root lengths of both WT and *piezo-cl* mutant seedlings were significantly reduced when the polarity of the MF was parallel to the direction of gravity under both red (Fig. S4C-F, S) and blue light (Fig. S4G-J, T). However, the root length was not significantly different in the WT and *piezo-cl* mutant seedlings when the polarity of the MF was anti-parallel to the direction of gravity under red light (Fig. S4K-N, U) and blue light (Fig. S4O-R, V). Compared with the root length of WT and *piezo-cl* mutant seedlings grown under blue light was significantly reduced (Fig.S4T) or no difference (Fig.S4V) when the polarity of the MF was parallel or anti-parallel to the direction of gravity, respectively, the root lengths of the WT was unchanged, but root length of *piezo-cl* mutants were significantly shorter when seedlings were grown under blue light and subjected to a MF with polarity perpendicular to the direction of gravity (Fig. 1O). These data indicate that *PIEZO* is sensitive to the polarity of MF under blue light when regulating root growth.

To check the effect of a MF on growth medium, which may then affect seedling root growth, 1/2 MS medium was subjected to a 500 mT MF for 6 days. Compared with seedlings grown in the 1/2 MS medium that was not subjected to a MF (Fig. S5A, D), the root lengths of both the

WT (Fig. S5B-C) and *piezo-cl* mutant (Fig. S5E-F) seedlings grown on the 1/2 MS medium previously subjected to a MF did not show significant differences under blue light (Fig. S5G).

We next checked whether *piezo* mutant seedling responses to MF regulation of root growth were dependent on the strength of the MF (Fig. S6A). Compared with the seedlings not subjected to a MF (Fig. S6B, E, H, K), the root length of WT (Fig. S6C-D) and *piezo-cl* mutant (Fig. S6F-G) seedlings did not show any significant differences when grown in a 50 mT MF under blue light (Fig. S6N). However, the root lengths were unchanged in the WT (Fig. S6I-J) but significantly reduced in the *piezo-cl* mutant seedlings (Fig. S6L-M) when grown in a 200 mT MF under blue light (Fig. S6O). These data show that the *PIEZO* gene regulates root growth in a MF strength-dependent manner under blue light.

***PIEZO* can perceive a blue light signal in a MF to regulate root growth**

We then assessed the effect of blue light in the regulation of the expression of the *PIEZO* gene. The *PIEZO* promoter contains different light responsive elements (Fig. S7, Table S2). In order to determine whether *PIEZO* is able to perceive a blue light signal transferred from the leaves to the roots, seedlings expressing *ProPIEZO::GUS* and subjected to a 500 mT MF were grown such that the leaves could receive blue light but the roots were in darkness (Fig. 2A). Under these conditions, GUS expression was detected in the cotyledon, hypocotyl, vascular tissue and root tip (Fig. 2B-C). Compared with the control seedlings not subjected to a MF (Fig. 2D), the levels of GUS in the root tips (Fig. 2E-F) were higher (Fig. 2G). In the WT seedlings grown such that the leaves received blue light but the roots were in darkness, expression levels of the *PIEZO* gene in the seedlings grown in a MF were higher than the control seedlings not subjected to a MF (Fig. 2H). This demonstrates that the *PIEZO* gene is able to perceive the blue light signal transferred from the leaves to roots in the presence of a MF.

***PIEZO* can regulate Ca^{2+} flux under MF and blue light treatment**

The *PIEZO* gene is known to regulate intracellular calcium ion transport in response to changes in perceived mechanical forces (Mousavi et al., 2021). To detect whether *PIEZO* regulation of root growth is related to Ca^{2+} flux, the real-time Ca^{2+} flux in WT and *piezo-cl* mutant seedlings grown under blue light in a 120 mT MF was investigated (Fig. S8). Compared with the control

seedlings not subjected to a MF, the Ca^{2+} flux in the roots of WT seedlings was unchanged (Fig. 3A). However, the Ca^{2+} efflux in the roots of *piezo-cl* mutant seedlings (Fig. 3B) grown in a MF under blue light was significantly reduced compared with the control. The above data show a good correlation with the root lengths of WT and *piezo-cl* mutant seedlings subjected to a 500 mT MF under blue light (Fig. 1O). To further investigate the effect of MF and blue light on the regulation of Ca^{2+} flux, WT and *piezo-cl* mutant seedlings were grown on 1/2 MS medium supplemented with 0.01 μM of the Ca^{2+} inhibitor ethylene glycol bis (2-aminoethyl ether)-N, N, N′, N′-tetraacetic acid (EGTA) in a 500 mT MF under blue light (Fig. 3C). Compared with seedlings not subjected to a MF, the primary root lengths of WT and *piezo-cl* mutant seedlings grown in a MF did not show any significant difference (Fig. 3D-J). These results suggest that the *PIEZO* gene is able to respond to MF and blue light to affect Ca^{2+} oscillation and modulate root growth.

PIEZO can modulate the effect of different phytohormones involved in root growth regulation

The root growth angles of *piezo-cl* mutant seedlings were affected when seedlings were subjected to a MF under blue light (Fig. 1R). To detect whether auxin, which is involved in root growth, has a role in the MF regulation of root growth in the *piezo-cl* mutant, WT and *piezo-cl* mutant seedlings were treated with the auxin transport inhibitor 2, 3, 5-triiodobenzoic acid (TIBA). The root lengths of WT seedlings grown on 1/2 MS medium complemented with DMSO as a control and subjected to a 500 mT MF under blue light (Fig. 4A) were not different from those in seedlings grown without a MF, while root lengths in the *piezo-cl* mutant were shorter (Fig. 4B-G, T). However, when seedlings were grown on 1/2 MS medium complemented with 5 μM TIBA in a MF under blue light, compared with the control grown without a MF, the primary root length remained unchanged in both the WT and the *piezo-cl* mutant (Fig. 4H-M, U). When the seedlings were grown on medium supplemented with 0.01 μM naphthalene-1-acetic acid (NAA) and subjected to a MF under blue light, compared to the control grown without a MF, the primary root length in the WT was unchanged, while it was increased in the *piezo-cl* mutant (Fig. 4N-S, V).

The function of *PIEZO* is connected to ethylene (Xu et al., 2024). Because a MF close to null decreases GA levels (Xu et al., 2016) and because the *PIEZO* promoter contains GA- and

MeJA-responsive elements (Fig. S7), we then detected the effects of GA, ethylene and MeJA on the regulation of root growth in *piezo-cl* mutant seedlings subjected to a 500 mT MF under blue light (Fig. S9A). When seedlings were treated with 0.1 μM 1- aminocyclopropane-1-carboxylic acid (ACC), which is a precursor of ethylene biosynthesis, compared with control seedlings grown on normal 1/2 MS medium and without MF treatment under blue light, no significant difference was detected in the the primary root lengths of WT seedlings, while root lengths were obviously reduced in the *piezo-cl* mutant seedlings subjected to a MF under blue light (Fig. S9B-G, AF). However, the primary root lengths of WT and *piezo-cl* seedlings did not show significant differences compared with the control grown without a MF when seedlings were treated with ACC and MF together under blue light (Fig. S9H-M, AG). Treatment with 10 μM GA4 also produced the same root phenotype as ACC (Fig. S9N-Y, AH-AI). However, the primary root lengths of WT and *piezo-cl* seedlings treated with 10 μM MeJA and grown in a MF were similar to those of the control treated with DMSO and grown in a MF under blue light (Fig. S9 N-S, Z-AE, AH, AJ).

CRY1 and 2 can respond to a MF to regulate root growth

The *PIEZO* gene is able to respond to a MF to regulate root growth in the presence of blue light (Fig. 1A-O). The blue light receptors CRY1 and 2 are also known to respond to a MF (Solov'yov et al., 2007; Agliassa et al., 2018) and affect auxin transport in root growth (Xu et al., 2018; Jin et al., 2019). To detect whether CRY1 and 2 are involved in MF-mediated root growth under blue light, the $cry_{1\text{-}104}$ and $cry_{2\text{-}1}$ single mutants and *cry1/2* double mutant were subjected to a 500 mT MF under blue light (Fig. 5A-M). Compared with the seedlings not subjected to a MF, the primary root lengths of WT seedlings grown in a MF under blue light were unchanged (Fig. 5B-D, N), but root lengths were significantly reduced compared to the control in the $cry_{1\text{-}104}$ (Fig. 5E-G, N) and $cry_{2\text{-}1}$ mutants (Fig. 5H-J, N). However, the primary root lengths of the *cry1/2* double mutant (Fig. 5K-M, N) did not show obvious change compared to the control. This suggests that the blue light signaling pathway is involved in the MF-mediation of root growth, and that the functions of *CRY1* and *2* are redundant in responding to MF. PIF3 is known to interact with PIEZO to regulate primary root growth (Bello-Bello and Herrera-Estrella, 2024; Xu et al., 2024). When *pif3* mutant seedlings were grown in a 500 mT MF under blue light, similar to the *piezo-cl* mutant (Fig. 1O), the primary root length of the *pif3* mutant was significantly

reduced compared with the control grown without a MF (Fig. S10).

PIEZO regulation of root growth in a MF and under blue light involves an integrated gene regulatory network

To gain insight into the mechanism of *PIEZO* regulation of root growth in a MF and under blue light, we analyzed WT and *piezo-cl* seedling root transcriptomes. A total of 1415 differentially expressed genes (DEGs) were found in the root transcriptomes (Table S1, Fig. S11). We found that these DEGs exhibited different expression patterns (Fig. S12), with a total of 1357 genes that specifically responded to blue light were identified in the *piezo-cl* mutant. To investigate the mechanism by which *PIEZO* responds to a MF and blue light, we first constructed an integrated gene regulatory network (iGRN) involving 237 genes by combining transcriptome data from this study, including protein-protein interaction data, miRNA regulation data, and transcription factor regulation data (Fig. S13). Next, we extracted a sub-network closely associated with *PIEZO* (Fig. 6A). Genes from the WT and *piezo-cl* root transcriptomes that had direct or indirect regulatory relationships with *PIEZO*, along with a microRNA m*iR5648-5p*, were identified as being involved in seven distinct biological processes, including auxin signaling, blue light signaling, calcium ion signaling, ethylene signaling, GA signaling, gravitropism, and mechanical pressure (Fig. 6A-B). To further validate the reliability of the dynamic expression changes of gene members in the sub-network, we next checked expression levels of DEGs in the sub-network using real-time PCR. The data showed that expression trends of 8 DEGs (Fig. 6C) were consistent with those of the transcriptome sequencing (Fig. 6B). Additionally, we examined the expression changes of the *miR5648-5p* shown in the sub-network (Fig. 6A), and found that the levels of m*iR5648-5p* were significantly decreased in the roots of WT grown in a 500 mT MF under blue light (Fig. 6D), which showed the opposite expression patterns of the *PIEZO* gene (Fig. 1S). This suggests that this microRNA is able to regulate the expression of *PIEZO* to affect root growth in a MF and under blue light. Based on the iGRN, we propose that *PIEZO* regulation of plant root growth in response to a MF and blue light involves certain phytohormones, including auxin, ethylene, and gibberellin, as well as calcium ion flux, gravity, mechanical pressure and miRNAs.

Discussion

The mechanosensitive protein PIEZO plays an important role in plant development. In this study, we found that the *PIEZO* gene could respond to the presence of a MF and blue light to regulate seedling root growth in *Arabidopsis*. PIEZO was able to respond to the direction of the MF polarity compared with the direction of gravity, and the expression of the *PIEZO* gene could be induced by an as yet unidentified signal transferred from the leaves to the roots. Under blue light and in a MF, PIEZO was able to affect Ca^{2+} flux associated with auxin, ethylene and gibberellin biosynthesis and signaling pathways, and miRNA.

MF affects plant development, and the regulation of root growth by *PIEZO* is related to the polarity of the MF, and whether this is perpendicular, parallel or anti-parallel to the direction of gravity (Fig. 1A, S4). PIEZO protein localizes to the vacuole membrane (Radin et al., 2021). However, how PIEZO perceives changes in MF polarity is unclear. The *PIEZO* gene regulates root growth dependent in blue light (Fig. 1B-O), and the blue light receptors CRY1 and 2 also can response to the presence of a MF to regulate root growth (Fig. 5). This implies that function of PIEZO is associated with the blue light signaling pathway as suggested in previous reports (Bello-Bello and Herrera-Estrella, 2024; Xu et al., 2024), and that either CRY1 or 2 is necessary for the plant to perceive a MF. However, whether and how PIEZO receives and responds to the blue light signal transferred from the leaves to roots is as yet unknown.

MF can modulate auxin transport to regulate root growth (Jin et al., 2019), and the regulation of root growth by the *PIEZO* gene is associated with Ca^{2+} flux (Fang et al., 2021). In this study, *PIEZO* was able to affect the Ca^{2+} efflux (Fig. 3) and auxin transport (Fig. 4) when seedlings were grown in a MF and under blue light. PIEZO localizes to the vascular tissue and root cap (Fig. 2B-F), which is a similar localization pattern to those of PIN3, PIN6 and PIN7 (Friml et al., 2002; Blilou et al., 2005; Benková et al., 2003). The iGRN (Fig. 6) contains LAZY2 and 4, which are involved in the response of root growth to gravity (Chen et al., 2023). This suggests that the root cap is the main area involved in the responses to both MF and gravity. Ca^{2+} signaling is associated with the regulation of root development by auxin (Wang et al., 2022; Leitão et al., 2019; Vanneste and Friml, 2013). Based on the iGRN (Fig. 6A), it is possible that PIEZO is able to regulate Ca^{2+} flux through mechanosensors, including MCA1 and 2, or the calcium related protein RCA, either directly or indirectly, and, moreover, indirectly to regulate auxin transport via ethylene-related genes.

The regulation of plant development by *PIEZO* involves different phytohormones (Hu et al., 2021). We demonstrated that although the phytohormones GA and ethylene are involved in the

regulation of *Arabidopsis* root growth by *PIEZO* in a MF and under blue light (Fig. S9), *PIEZO* did not directly regulate or interact with the GA-related genes, with the exception of the ethylene-related genes (Fig. 6A). A near-null MF can affect the expression of GA-related genes (Xu et al., 2016), although in our study, the GA-related genes did not show a differential expression pattern in the *piezo-cl* mutant (Fig. 6A), the effect of GA4 in the regulation of the root growth of *piezo-cl* mutant in a MF and under blue light (Fig. S9AH-AI) may be involved in an unknown pathway, or that a 500 mT MF affects the expression patterns of GA-related genes that may be linked with the mutation of the *PIEZO* gene. Moreover, ethylene may regulate root growth in the *piezo-cl* mutant via the *PIF3* gene, as reported previously (Xu et al., 2024). Importantly, the expression of miRNA were also affected by the presence of a MF and could negatively regulate the expression of the *PIEZO* gene (Fig. 6A, D). This suggests certain upstream genes also participate in regulation of root growth by *PIEZO* in a MF and under blue light.

PIEZO not only perceives mechanical force but can also respond to MF and blue light. Further studies will focus on investigating how PIEZO is able to perceive MF polarity, and on elucidating the connection between PIEZO and CRY1 and 2. Of particular interest is the mechanism underlying miRNA detection of the MF and regulation of the expression of *PIEZO*. This study demonstrates the regulation of root growth by *PIEZO* via an uncommon mechanism involving the perception of both MF and blue light, and provides fresh insights into how the Earth's MF and blue light together regulate plant development.

Figures and legends

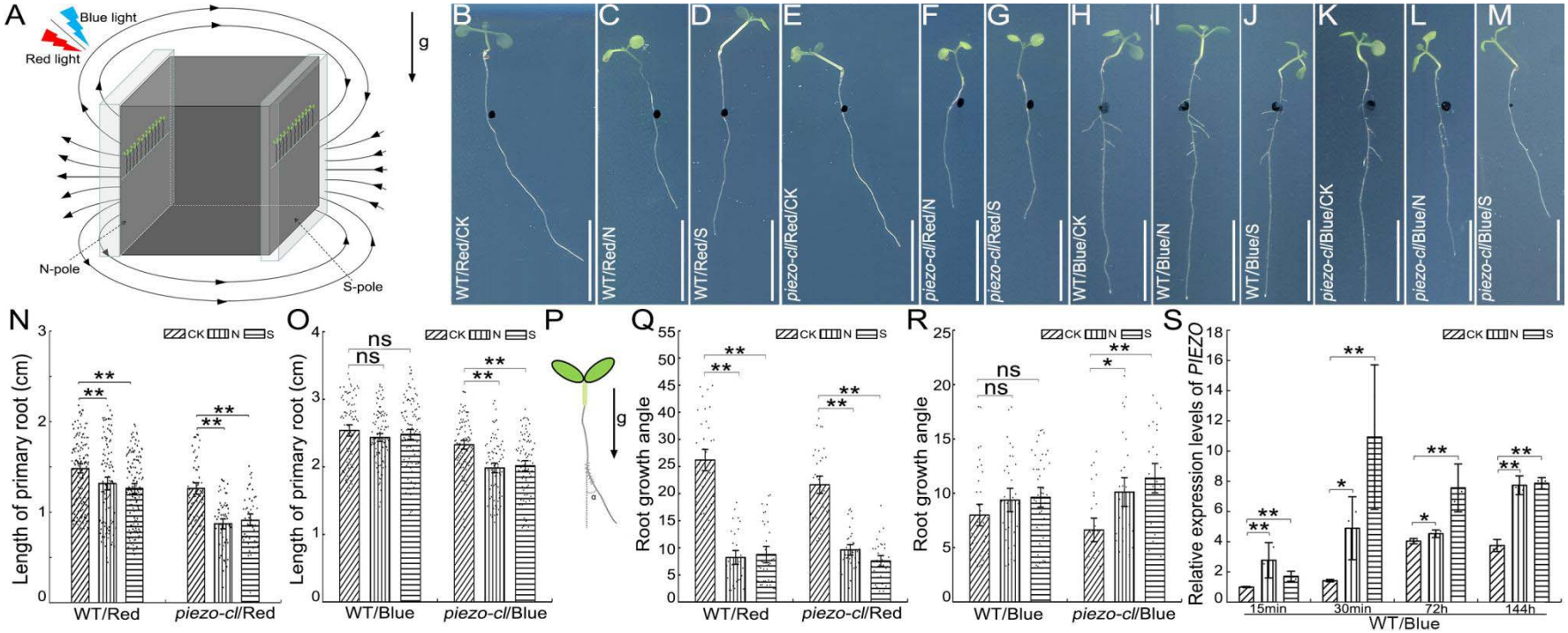

Fig. 1 Root phenotypes and *PIEZO* expression in WT and *piezo-cl* mutant seedlings subjected to a MF under red or blue light.

Schematic diagram of *Arabidopsis* seedlings subjected to a MF under blue or red light (A). The root phenotypes of WT and *piezo-cl* mutant seedlings treated with 500 mT MF under red light (B-G) and blue light (H-M). Quantification of the primary root length of WT and *piezo-cl* mutant seedlings in a MF under red light (N) (WT: n_{CK}=120, n_N=105, n_S=127; *piezo-cl*: n_{CK}=56, n_N=60, n_S=48) or blue light (O) (WT: n_{CK}=82, n_N=102, n_S=106; *piezo-cl*: n_{CK}=87, n_N=82, n_S=83). Schematic diagram of root growth angle when seedlings were subjected to a MF showing the root response to gravity (P). Quantification of the root growth angle (α) of WT and *piezo-cl* mutant seedlings under red light (Q) (WT: n_{CK}=36, n_N=31, n_S=33; *piezo-cl*: n_{CK}=35, n_N=34, n_S=32) or blue light (R) (WT: n_{CK}=37, n_N=33, n_S=43;

piezo-cl: n_{CK}=26, n_N=29, n_S=26). Expression levels of the *PIEZO* gene in WT seedlings at different times following onset of treatment (15 min, 30 min, 72 hr, and 144 hr) and subjected to a 500 mT MF under blue light (S). The *AtActin2* gene was used as an internal control. Data are means ± SE (Image N-O, Q-R). Arrows labeled "g" indicate the direction of gravity; the black, curved and solid lines with arrow heads represent the direction of the MF lines. The black dotted lines point to the N or S pole of the magnetic block, respectively. WT = wild-type. CK = seedlings not subjected to a MF, N = seedlings treated with the N pole of the magnetic block, S = seedlings treated with the S pole of the magnetic block. Blue = Seedlings treated with blue light. Red = Seedlings treated with red light. Data are means ± SD (Image S), the data presented here represent at least three biological replicates. ns = not significant, * $P < 0.05$, ** $P < 0.01$ (Student's *t*-test). Scale bar = 1 cm.

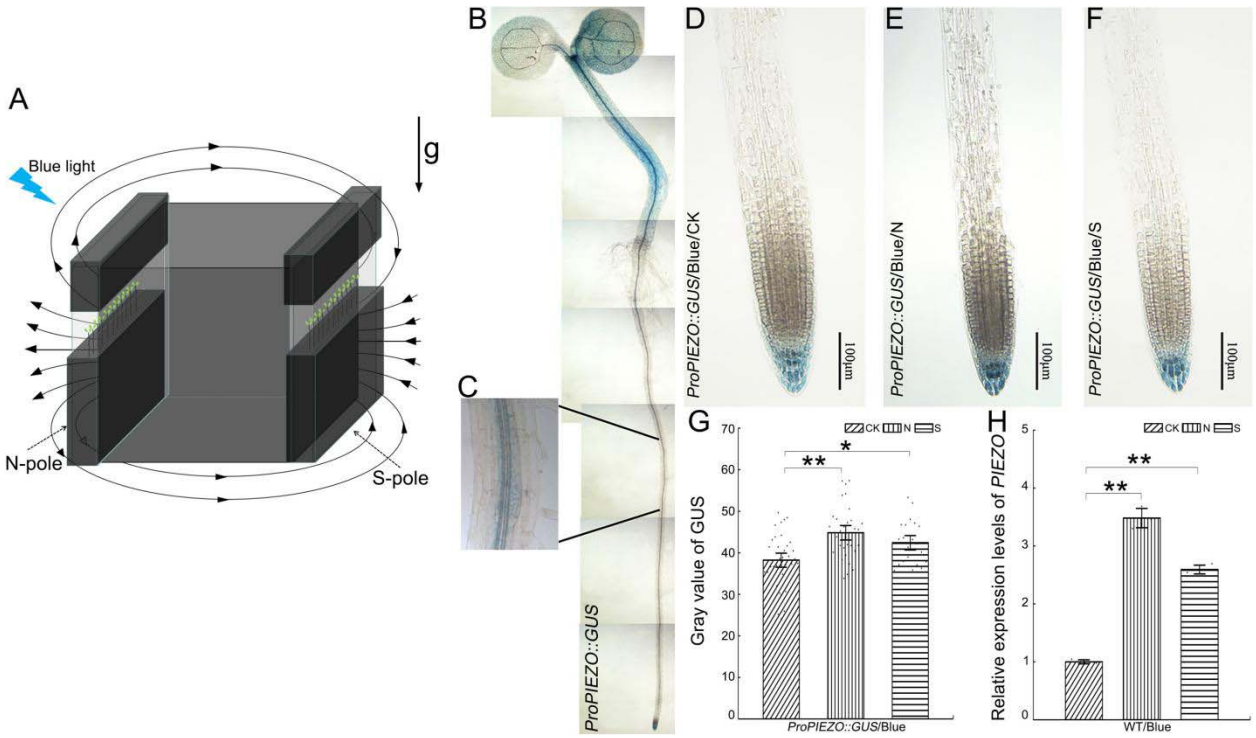

Fig. 2 Expression patterns of the *GUS* and *PIEZO* genes in seedlings subjected to a MF under blue light.

Schematic diagram of seedlings expressing *ProPIEZO::GUS* subjected to a MF under blue light (A). Expression patterns of GUS in 10-day-old seedlings expressing *ProPIEZO::GUS* (B-C). The GUS expression in the root cap of seedlings expressing *ProPIEZO::GUS* without MF (D) or with 500 mT MF (E-F) under blue light. Quantification of GUS intensity (G) in root tips (n_{CK}=34, n_N=31, n_S=21). Data are means ± SE (in image G). Expression levels of *PIEZO* gene in the roots of WT seedlings with MF treatment under blue light (H). The *AtActin2* gene was used as an internal control. Arrows labeled "g" indicate the direction of gravity; the black, curved and solid lines with arrow heads represent the direction of the MF lines. The black dotted lines point to the N or S pole of the magnetic block, respectively. WT = wild-type. CK = seedlings not subjected to a MF, N = seedlings treated with the N pole of the magnetic block, S = seedlings treated with the S pole of the magnetic block. Blue = Seedlings treated with blue light. Data are means ± SD (in image H), the data presented here represent at least three biological replicates. ns = not significant, * $P < 0.05$, ** $P < 0.01$ (Student's *t*-test).

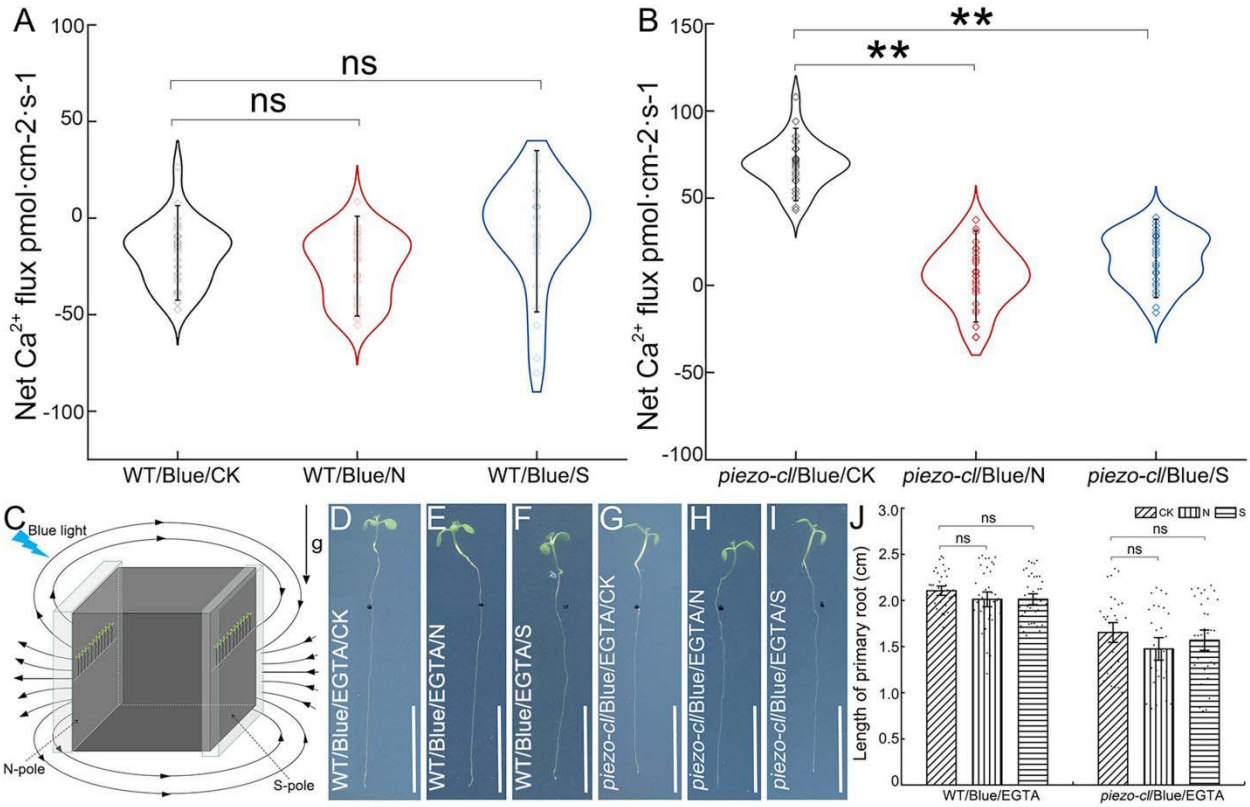

Fig. 3 Calcium ion flux in the root tips of WT and *piezo-cl* mutant seedlings subjected to a MF under blue light.

Ca^{2+} flux in the root tips of WT (A) (n_{CK} = 29, n_N = 29, n_S = 29) and *piezo-cl* mutant (B) seedlings (n_{CK} = 29, n_N = 29, n_S = 29) subjected to a 500 mT MF under blue light. Data are means ± SD (in image A-B). Schematic diagram of seedlings subjected to MF under blue light (C). The root phenotype of WT (D-F) and *piezo-cl* mutant seedlings (G-I) grown on 1/2 MS medium supplemented with 0.01 μM EGTA not subjected to a MF (D, G) or subjected to a 500 mT MF (E-F, H-I) under blue light (D-I). Quantification of the primary root length of WT and *piezo-cl* mutant seedlings (J) (WT: n_{CK}=39, n_N=38, n_S=40; *piezo-cl*: n_{CK}=32, n_N=29, n_S=34). Arrows labeled "g" indicate the direction of gravity; the black, curved and solid lines with arrow heads represent the direction of the MF lines. The black dotted lines point to the N or S pole of the magnetic block, respectively. WT = wild-type. CK = seedlings not subjected to a MF, N = seedlings treated with the N pole of the magnetic block, S = seedlings treated with the S pole of the magnetic block. Blue = Seedlings treated with blue light. Data are means ± SE (in image J). ns = not significant, ** $P < 0.01$ (Student's *t*-test). Scale bar = 1 cm.

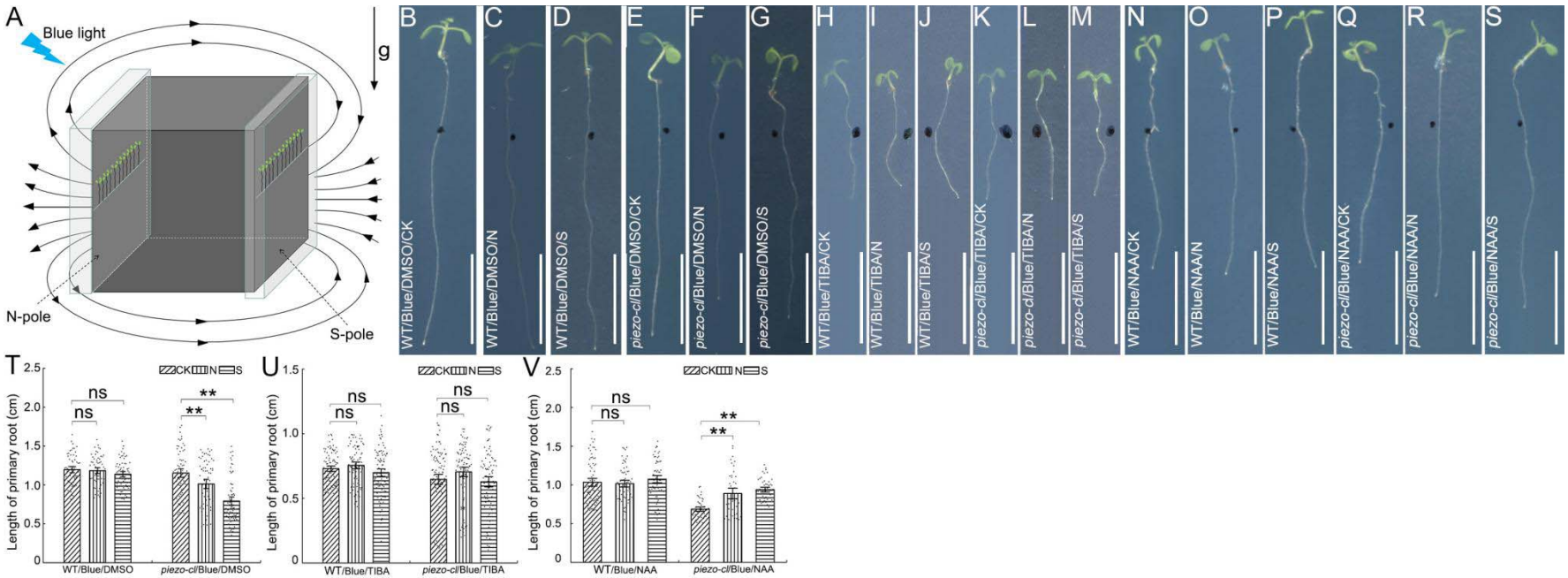

Fig. 4 Root phenotypes of *piezo-cl* mutant seedlings treated with an auxin transport inhibitor and grown in a MF under blue light.

Schematic diagram of seedlings subjected to a MF under blue light (A). The root phenotypes of WT (B-D, H-J, N-P) and *piezo-cl* mutant (E-G, K-M, Q-S) seedlings grown on 1/2 MS supplemented with DMSO as a control (B-G), 5 μM TIBA (H-M) or 0.01 μM NAA (N-S) without MF (B, E, H, K, N, Q) or 500 mT MF (C-D, F-G, I-J, L-M, O-P, R-S) under blue light (B-S). Quantification of the primary root length of WT and *piezo-cl* mutant seedlings treated with DMSO (T) (WT: n_{CK}=58, n_N=59, n_S=64; *piezo-cl*/Blue/DMSO: n_{CK}=67, n_N=65, n_S=69), 5 μM TIBA (U) (WT: n_{CK}=86, n_N=83, n_S=94; *piezo-cl*: n_{CK}=97, n_N=87, n_S=86) and 0.01 μM NAA (V) (WT: n_{CK}=72, n_N=63, n_S=63; *piezo-cl*: n_{CK}=46, n_N=40, n_S=47). Arrows labeled “g” indicate the direction of gravity; the black, curved and solid lines with arrow heads represent the direction of the MF lines. The black dotted lines point to the N or S pole of the magnetic block, respectively. WT = wild-type. CK = seedlings not subjected to a MF, N = seedlings treated with the N pole of the magnetic block, S = seedlings treated with

the S pole of the magnetic block. Blue = Seedlings treated with blue light. The data presented here represent at least three biological replicates. Data are means ± SE. ns = not significant, * $P < 0.05$, ** $P < 0.01$ (Student's *t*-test). Scale bar = 1 cm.

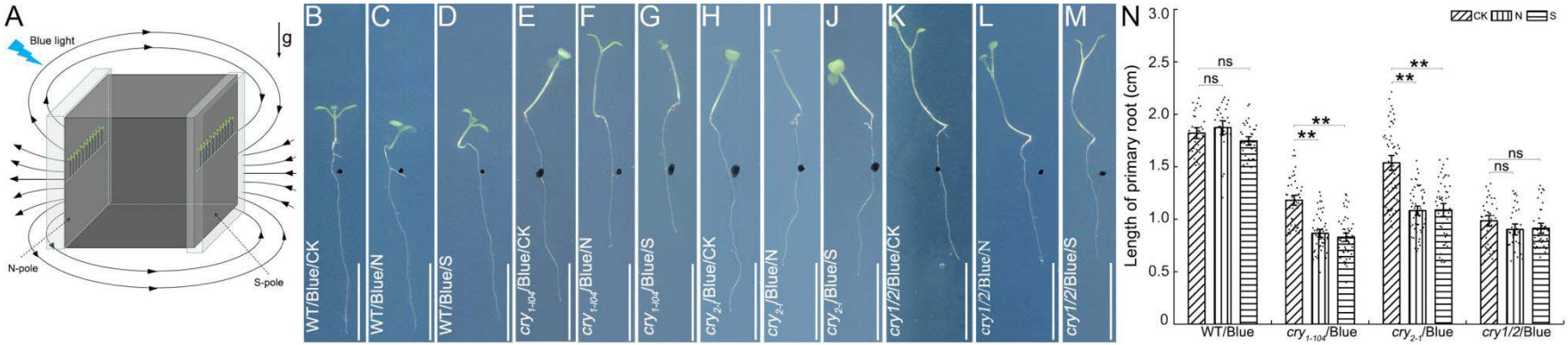

Fig. 5 Root phenotypes of *cry1* and *2* mutant line seedlings subjected to a MF under blue light.

Schematic diagram of seedlings subjected to a MF under blue light (A). The root phenotypes of WT (B-D), *cry*$_{1\text{-}104}$ mutant (E-G), *cry*$_{2\text{-}1}$ mutant (H-J) and *cry1/2* mutant (K-M) seedlings not subjected to a MF (B, E, H, K) or subjected to a 500 mT MF (C-D, F-G, I-J, L-M) under blue light (B-M). Quantification of the primary root length of WT, *cry*$_{1\text{-}104}$, *cry*$_{2\text{-}1}$ and *cry1/2* mutant seedlings (N) (WT: n_{CK}=30, n_N=30, n_S=36; *cry*$_{1\text{-}104}$: n_{CK}=47, n_N=51, n_S=53; *cry*$_{2\text{-}1}$: n_{CK}=55, n_N=56, n_S=54; *cry1/2*: n_{CK}=36, n_N=34, n_S=37). Arrows labeled "g" indicate the direction of gravity; the black, curved and solid lines with arrow heads represent the direction of the MF lines. The black dotted lines point to the N or S pole of the magnetic block, respectively. WT = wild-type. CK = seedlings not subjected to a MF, N = seedlings treated with the N pole of the magnetic block, S = seedlings treated with the S pole of the magnetic block. Blue = Seedlings treated with blue light. Data are means ± SE, ns = not significant, ** $P < 0.01$ (Student's *t*-test). Scale bar = 1 cm.

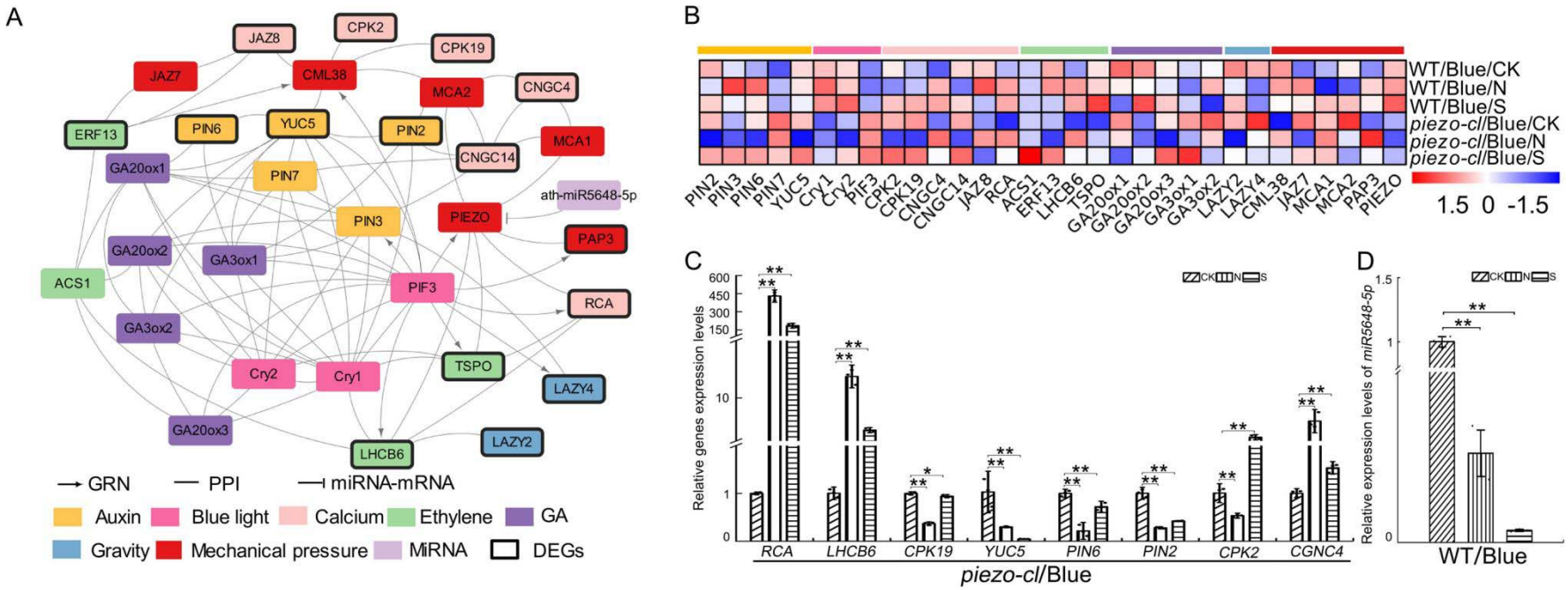

Fig. 6 The sub-network of iGRN associated with *PIEZO*.

The integrated network of MF-responsive and blue light-responsive genes includes the protein interaction network (PPI), transcription factor regulatory network (GRN) and miRNA-targets regulatory network (miRNA-mRNA) (A). Heatmap showing the normalized FPKM values of unigenes in the sub-network (B). Expression levels of *Arabidopsis* unigenes from the sub-network (C) and *miR5648-5p* (D) in seedlings subjected to a 500 mT MF under blue light. The *AtActin2* gene was used as an internal control. WT = wild-type. CK = seedlings not subjected to a MF, N = seedlings treated with the N pole of the magnetic block, S = seedlings treated with the S pole of the magnetic block. Blue = Seedlings treated with blue light. Data are means ± SD. The data presented here represent at least three biological replicates. * $P < 0.05$, ** $P < 0.01$ (Student's *t*-test).

Supplemental data

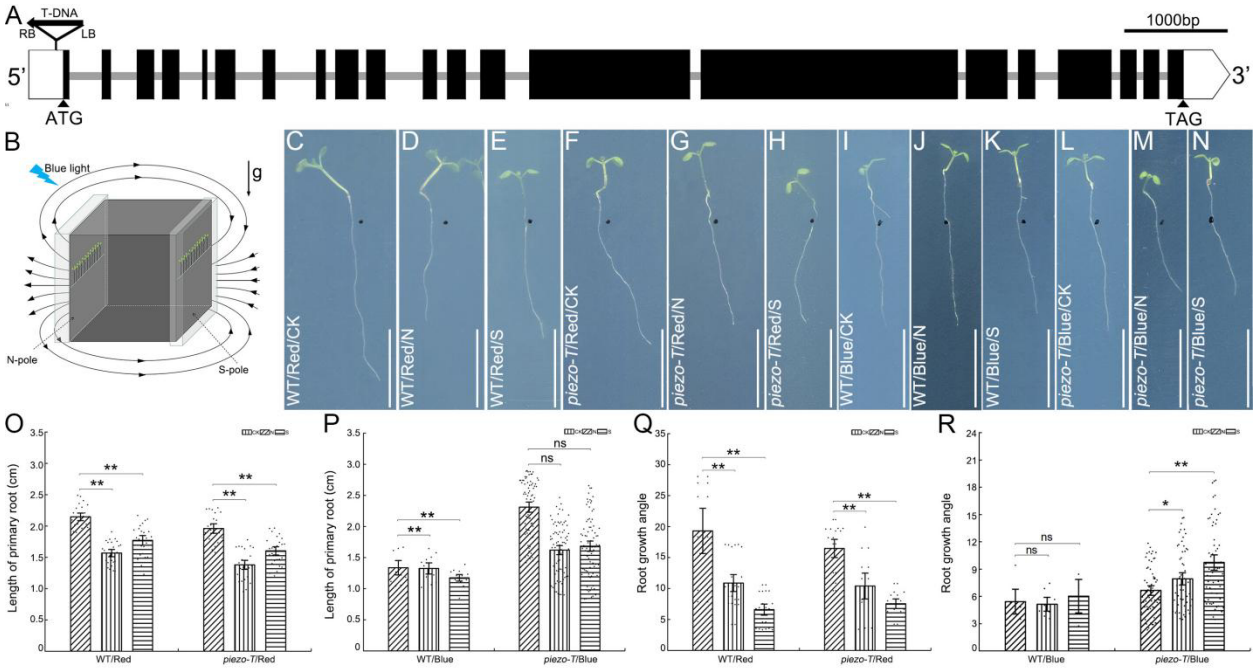

Fig. S1 Root phenotypes of *piezo-T* mutant seedlings subjected to a MF under blue light.

Schematic diagram of the *PIEZO* gene with a T-DNA insertion (A). Schematic diagram of seedlings subjected to a MF under blue light (B). The root phenotypes of WT (C-E, I-K) and *piezo-T* mutant (F-H, L-N) seedlings without a MF (C, F, I, L) or with a 500 mT MF treatment (D-E, G-H, J-K, M-N) under red light (C-H) or blue light (I-N). Quantification of the primary root length of WT and *piezo-T* mutant seedlings under MF treatment and grown under red light (O) (WT: n_{CK}=22, n_N=24, n_S=24; *piezo-T*: n_{CK}=22, n_N=25, n_S=26) or blue light (P) (WT: n_{CK}=10 n_N=12, n_S=13; *piezo-T*: n_{CK}=73, n_N=78, n_S=80). Quantification of the root growth angle (α) of WT and *piezo-T* mutant seedlings under MF treatment and grown under red light (Q) (WT: n_{CK}=12, n_N=22, n_S=20; *piezo-T*: n_{CK}=18, n_N=14, n_S=16) or blue light (R) (WT: n_{CK}=6, n_N=8, n_S=4; *piezo-T*: n_{CK}=60, n_N=56, n_S=58). Black boxes indicate exons, white boxes indicate 5' UTR and 3' UTR, gray lines indicate introns, triangle indicates T-DNA insertion sites and the arrow head shows the direction of T-DNA insertion, and the filled triangles indicate the initiation codon ATG and termination codon TAG, respectively. Arrows labeled “g” indicate the direction of gravity; the black, curved and solid lines with arrow heads represent the direction of the MF lines. The black dotted lines point to the N or S pole of the magnetic block, respectively. LB = the left border of T-DNA, RB = the right border of T-DNA. WT = wild-type. CK = seedlings not subjected to a MF, N = seedlings treated with the N pole of the magnetic block, S = seedlings

treated with the S pole of the magnetic block. Blue = Seedlings treated with blue light. Data are means ± SE. ns = not significant, * $P < 0.05$, ** $P < 0.01$ (Student's *t*-test). Scale bar = 1 cm.

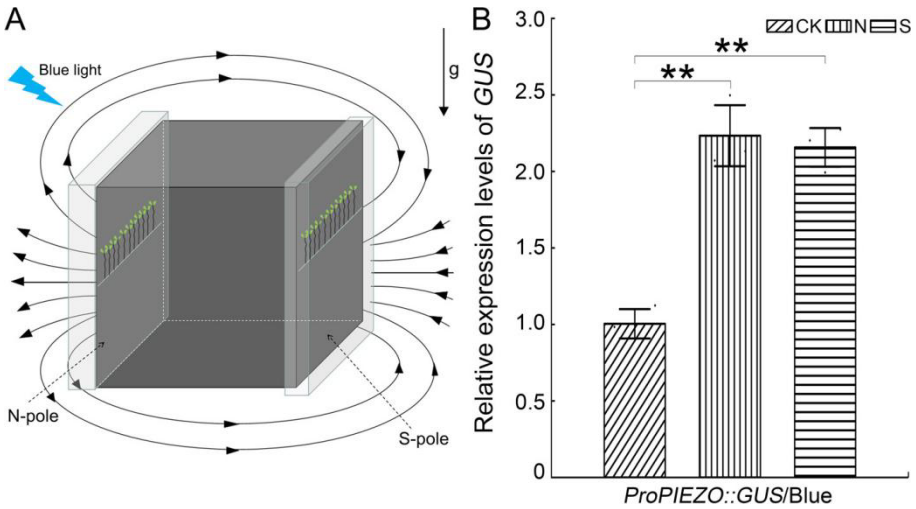

Fig. S2 Expression levels of *GUS* gene in *Arabidopsis* seedlings subjected to a MF under blue light.

Schematic diagram of seedlings subjected to a MF under blue light (A). (B) Expression levels of the *GUS* gene in the roots of seedlings expressing *ProPIEZO::GUS* in a 500 mT MF under blue light. The *AtActin2* gene was used as an internal control. Arrows labeled "g" indicate the direction of gravity; the black, curved and solid lines with arrow heads represent the direction of the MF lines. The black dotted lines point to the N or S pole of the magnetic block, respectively. WT = wild-type. CK = seedlings not subjected to a MF, N = seedlings treated with the N pole of the magnetic block, S = seedlings treated with the S pole of the magnetic block. Blue = Seedlings treated with blue light. Data are means ± SD. The data presented here represent at least three biological replicates. ** $P < 0.01$ (Student's *t*-test).

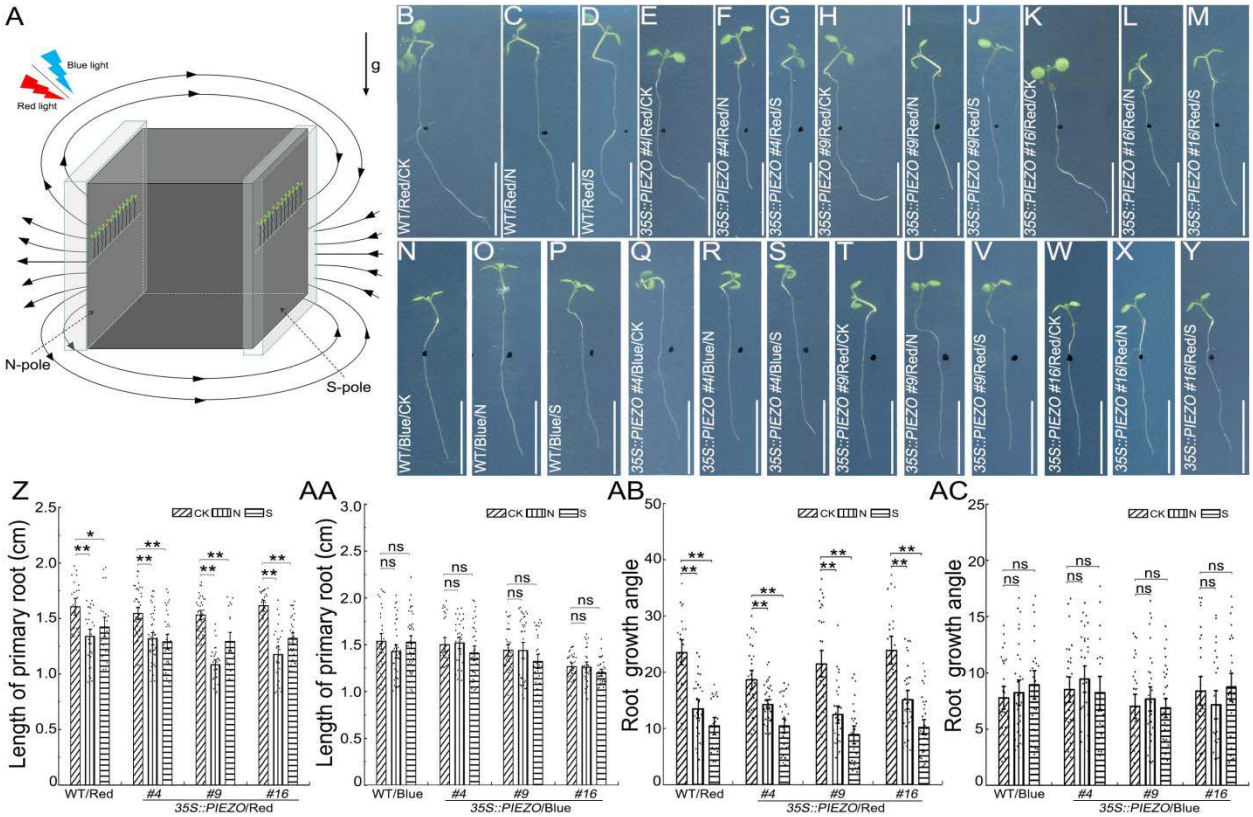

Fig. S3 Root phenotypes of seedlings from *35S::PIEZO* lines in a MF under red or blue light.

Schematic diagram of seedlings subjected to a MF under blue or red light (A). The root phenotypes of WT (B-D, N-P) and *35S::PIEZO* lines #4 (E-G, Q-S), #9 (H-J, T-V), #16 (K-M, W-Y) not subjected to a MF (B, E, H, K, N, Q, T, W) or in a 500 mT MF (C-D, F-G, I-J, L-M,O-P, R-S, U-V, X-Y) under red light (B-M) or blue light (N-Y). Quantification of the primary root length of WT and *35S::PIEZO* lines #4, #9, #16 subjected to a MF under red light (Z) (WT: n_{CK}=23, n_N=30, n_S=23; #4: n_{CK}=41, n_N=42, n_S=33; #9: n_{CK}=36, n_N=29, n_S=21; #16: n_{CK}=24, n_N=26, n_S=33) or blue light (AA) (WT: n_{CK}=33, n_N=39, n_S=41; #4: n_{CK}=28, n_N=34, n_S=35; #9: n_{CK}=31, n_N=37, n_S=33; #16: n_{CK}=31, n_N=29, n_S=32). Quantification of the root growth angle (α) in seedlings of WT and *35S::PIEZO* lines #4, #9, #16 subjected to a MF under red light (AB) (WT: n_{CK}=22, n_N=27, n_S=21; #4: n_{CK}=31, n_N=36, n_S=30; #9: n_{CK}=32, n_N=29, n_S=26; #16: n_{CK}=23, n_N=31, n_S=34) or blue light (AC) (WT: n_{CK}=27, n_N=30, n_S=25; #4: n_{CK}=28, n_N=31, n_S=21; #9: n_{CK}=29, n_N=32, n_S=33; #16: n_{CK}=29, n_N=26, n_S=28). Arrows labeled “g” indicate the direction of gravity; the black, curved and solid lines with arrow heads represent the direction of the MF lines. The black dotted lines point to the N or S pole of the magnetic block, respectively. WT = wild-

type. CK = seedlings not subjected to a MF, N = seedlings treated with the N pole of the magnetic block, S = seedlings treated with the S pole of the magnetic block. Blue = Seedlings treated with blue light. Red = Seedlings treated with red light. Data are means ± SE. ns = not significant, * $P < 0.05$, ** $P < 0.01$ (Student's *t*-test).

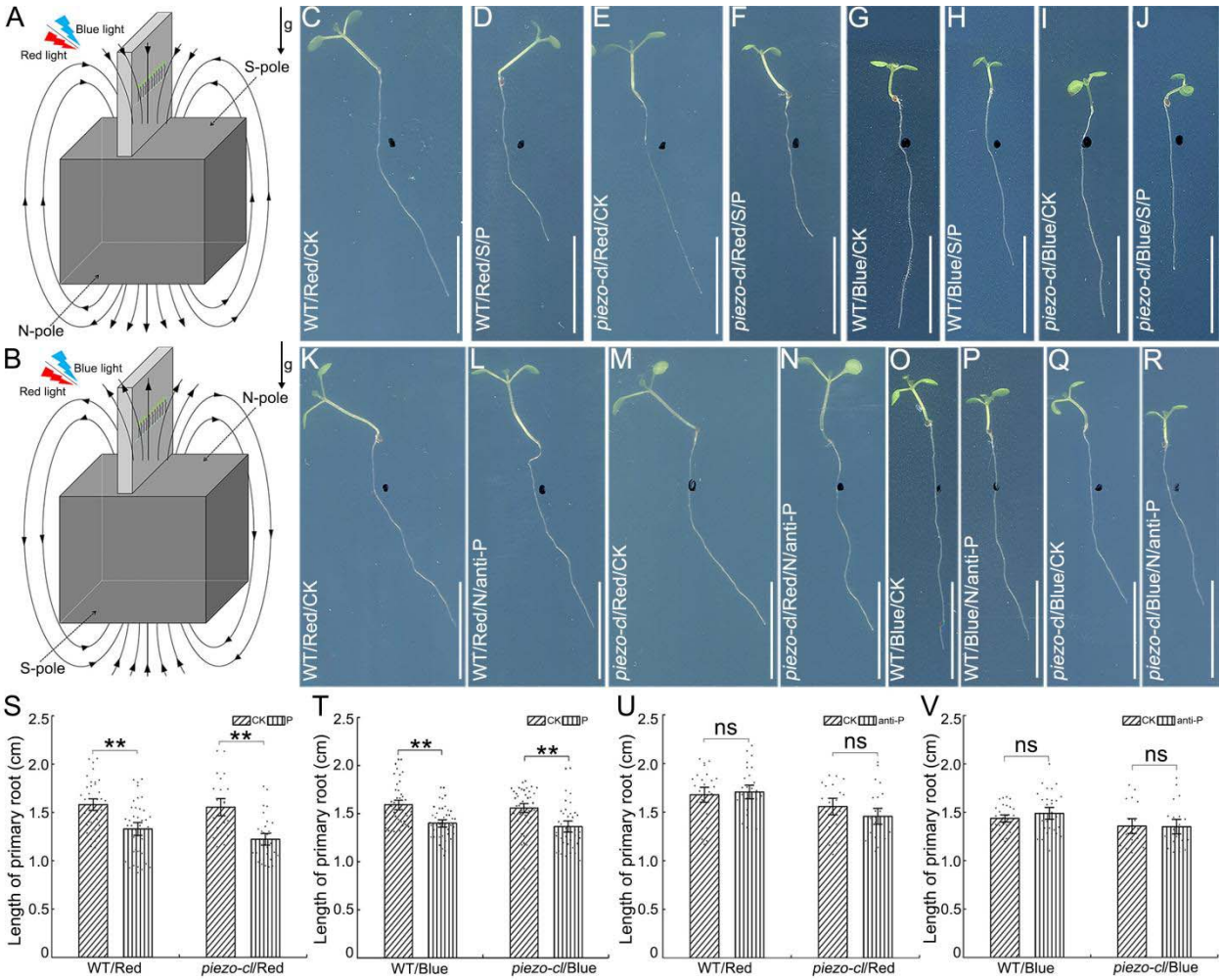

Fig. S4 Root phenotypes of *piezo-cl* mutant seedlings subjected to a MF in parallel and anti-parallel with gravity under red or blue light.

Schematic diagram of seedlings subjected to a MF in parallel (A) or anti-parallel (B) with the direction of gravity under blue or red light. The root phenotypes of WT (C-D, G-H, K-L, O-P) and *piezo-cl* mutant (E-F, I-J, M-N, Q-R) seedlings subjected to a 500 mT MF parallel to the direction of gravity (C-J) or anti-parallel to the direction of gravity (K-R) under red light (C-F, K-N) or blue light (G-J, O-R). (S) Quantification of the primary root length of WT and *piezo-cl* mutant seedlings subjected to a MF in parallel to the direction of gravity under red light (S) (WT: n_{CK}=39, n_G=40; *piezo-cl*: n_{CK}=24, n_G=32) or blue light (T) (WT: n_{CK}=42, n_G=45; *piezo-cl*: n_{CK}=49, n_G=38). Quantification of the primary root length of WT and *piezo-cl* mutant seedlings subjected to a MF in anti-parallel to the direction of gravity under red light (U) (WT: n_{CK}=26, $n_{Anti\text{-}G}$=27; *piezo-cl*: n_{CK}=20, $n_{Anti\text{-}G}$=24) or blue light (WT: n_{CK}=29, $n_{Anti\text{-}G}$=29; *piezo-cl*: n_{CK}=19, $n_{Anti\text{-}G}$=21). Arrows labeled “g” indicate the direction of gravity; the black, curved and solid lines

with arrow heads represent the direction of the MF lines. The black dotted lines point to the N or S pole of the magnetic block, respectively. WT = wild-type. CK = seedlings not subjected to a MF, N = seedlings treated with the N pole of the magnetic block, S = seedlings treated with the S pole of the magnetic block. Blue = Seedlings treated with blue light. Red = Seedlings treated with red light. P = the direction of the MF is parallel to the direction of gravity, anti-P = the direction of MF is anti-parallel to the direction of gravity. Data are means ± SE. ns = not significant, * $P < 0.05$, ** $P < 0.01$ (Student's *t*-test). Scale bar = 1 cm.

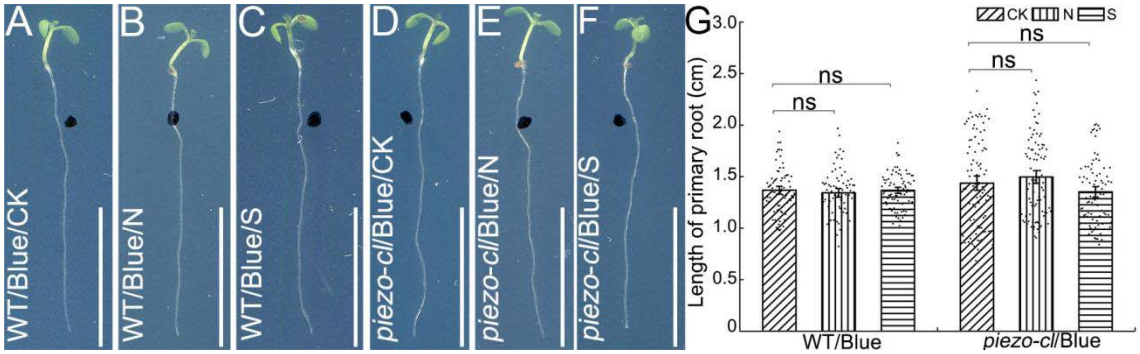

Fig.S5 Root phenotypes of *piezo-cl* mutant seedlings grown on MF pre-treated medium under blue light.

Root phenotypes of 6-day-old seedlings of WT (A-C) and *piezo-cl* mutant (D-F) seedlings grown on 1/2 MS medium without MF treatment (A, D) or pre-treated with 500 mT MF (B-C, E-F) under blue light (A-F). Quantification of the primary root length of WT and *piezo-cl* mutant (G) seedlings (WT: n_{CK}=76, n_N=70, n_S=77; *piezo-cl*: n_{CK}=92, n_N=91, n_S=85). WT = wild-type. CK = 1/2 MS medium without MF treatment, N = 1/2 MS medium was pre-treated with the N pole of the magnetic block, S = 1/2 MS medium was pre-treated with the S pole of the magnetic block. Blue = Seedlings treated with blue light. Data are means ± SE. ns = not significant. Scale bar = 1 cm.

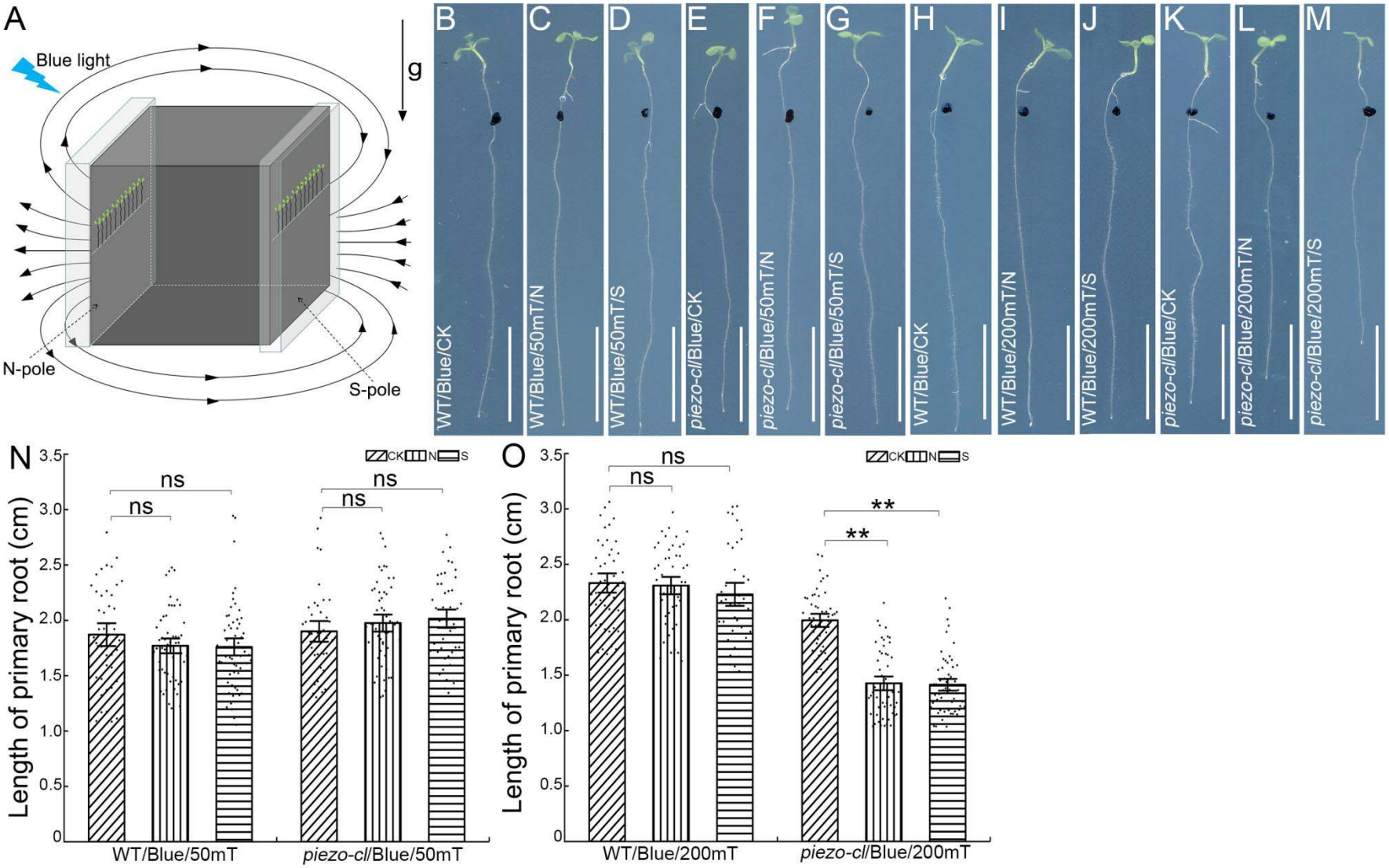

Fig.S6 Root phenotypes of *piezo-cl* mutant seedlings subjected to different MF intensities under blue light.

Schematic diagram of seedlings subjected to a MF under blue light (A). The root phenotypes of 6-day-old seedlings of WT (B-D, H-J) and *piezo-cl* mutant lines (E-G, K-M) not subjected to a MF (B, E, H, K) or subjected to a 50 mT MF (C-D, F-G) or a 200 mT MF (I-J, L-M) under blue light (B-M). Quantification of the primary root length of WT and *piezo-cl* mutant seedlings subjected to a 50 mT MF (N) (WT: n_{CK}=43, n_N=54, n_S=58; *piezo-cl*: n_{CK}=40, n_N=54, n_S=46) or a 200 mT MF (O) (WT: n_{CK}=44, n_N=48, n_S=39; *piezo-cl*: n_{CK}=50, n_N=53, n_S=57). Arrows labeled "g" indicate the direction of gravity; the black, curved and solid lines with arrow heads represent the direction of the MF lines. The black dotted lines point to the N or S pole of the magnetic block, respectively. WT = wild-type. CK = seedlings not subjected to a MF, N = seedlings treated with the N pole of the magnetic block, S = seedlings treated with the S pole of the magnetic block. Blue = Seedlings treated with blue light. Data are means ± SE. ns = not significant, ** $P < 0.01$ (Student's *t*-test). Scale bar = 1 cm.

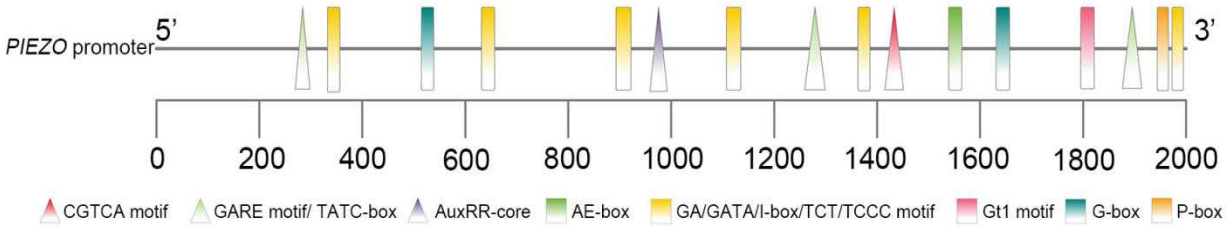

Fig.S7 Structure of the *Arabidopsis PIEZO* promoter.

The *Arabidopsis PIEZO* promoter contains eight light responsive elements comprising an AE-box (AGAAACTT), GA motif (ATAGATAA), GATA motif (AAGGATAAGG), I-box motif (GGATAAGGTG), TCT motif (TCTTAC), TCCC motif (TCTCCCT), Gt1 motif (GTGTGTGAA), and G-box (TACGTG/CACGAC); an auxin responsive element comprising an AuxRR-core (GGTCCAT); three GA responsive element comprising a P-box (CCTTTTG), GARE motif (TCTGTTG), TATC-box (TATCCCA); and a MeJA responsive element comprising a CGTCA-motif (CGTCA).

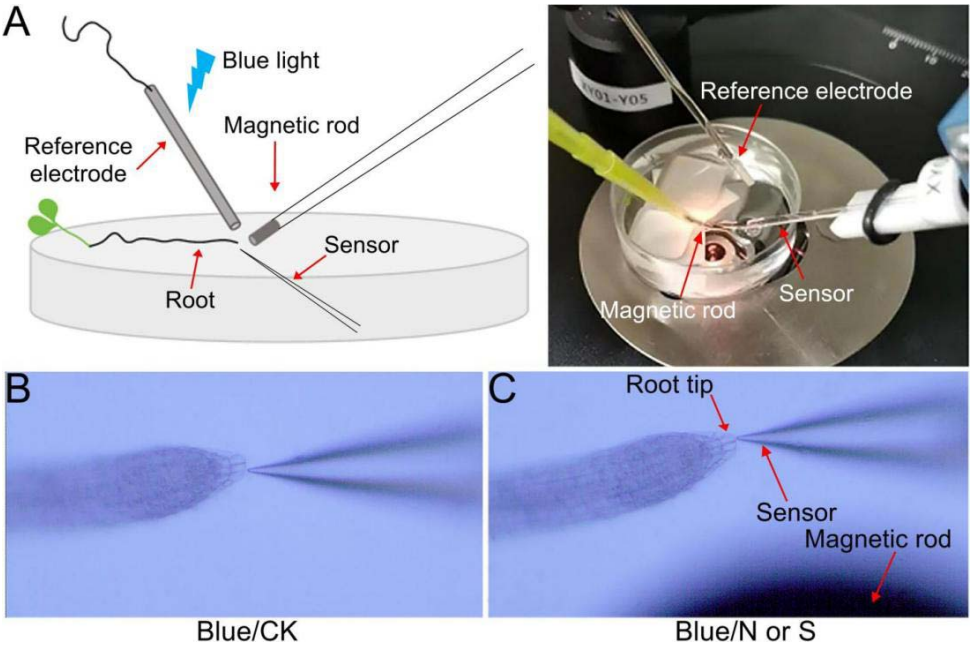

Fig.S8 Schematic diagram of calcium ion measurement in the root tips of *piezo-cl* mutant seedlings subjected to a MF under blue light.

The roots of seedlings of WT and *piezo-cl* mutants were fixed in 0.1 mM $CaCl_2$ solution and treated with the 120 mT magnetic rod under blue light. The Ca^{2+} flux rate in the root tip was determined in real-time using a sensor (A). The Ca^{2+} flux in the root tips of seedlings not subjected to MF (B) or treated with a magnetic rod (C) under blue light and detected using a sensor. The black zone is the image of magnetic rod seen under the microscope. Blue = Roots of seedlings treated with blue light. WT = wild-type. CK = Roots of seedlings without magnetic rod treatment, N = Roots of seedlings treated with the N pole of the magnetic rod, S = Roots of seedlings treated with the S pole of the magnetic rod.

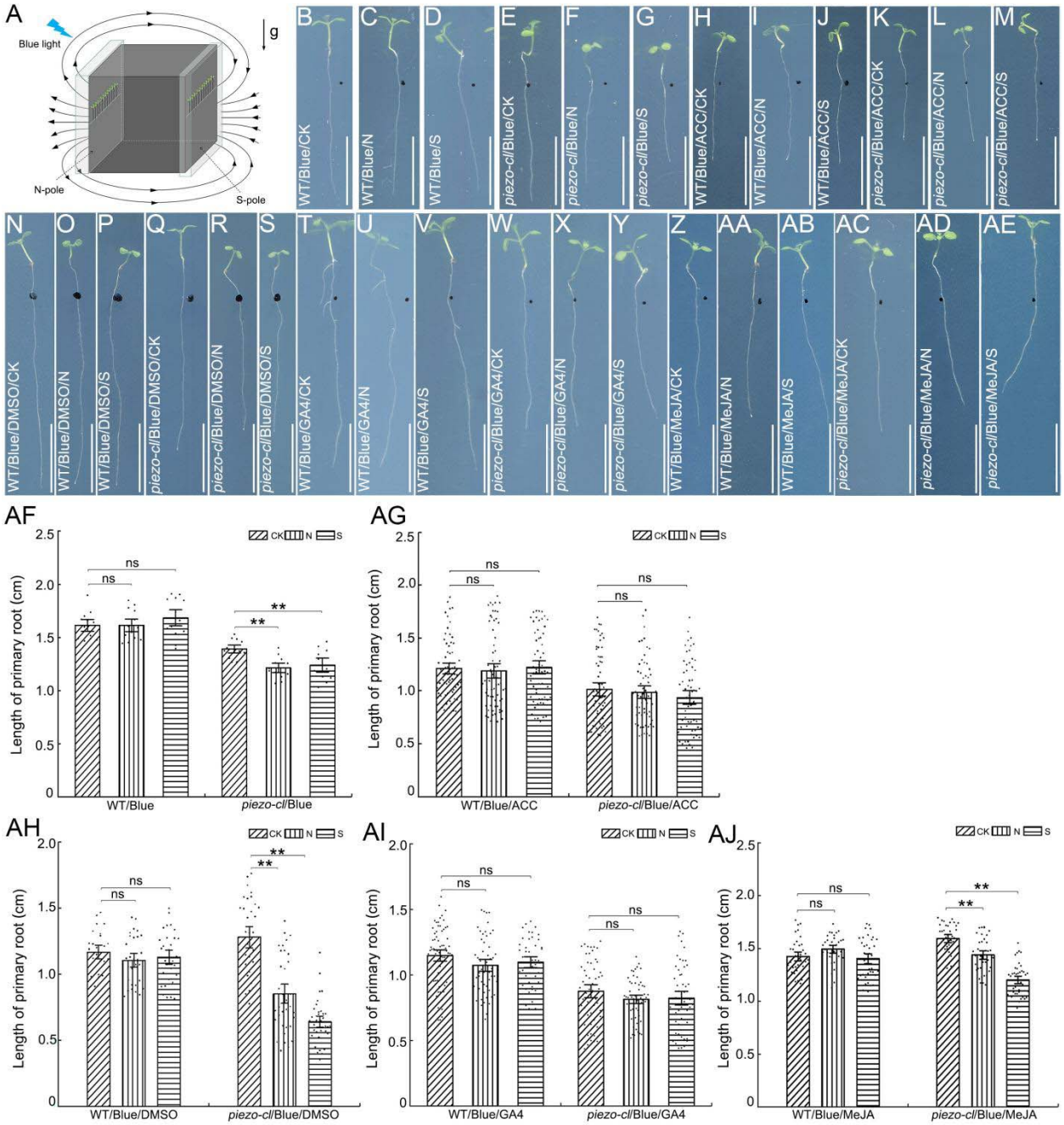

Fig. S9 Root phenotypes of *piezo-cl* mutant seedlings treated with ACC, GA4, MeJA and MF under blue light.

Schematic diagram of seedlings subjected to a MF under blue light (A). The root phenotypes of WT (B-D, H-J, N-P, T-V, Z-AB) and *piezo-cl* mutant (E-G, K-M, Q-S, W-Y, AC-AE) seedlings grown on 1/2 MS medium (B-G) as a control, or on 1/2 MS medium supplemented with 0.1 μM ACC (H-M), or 1/2 MS medium supplemented with DMSO (N-S) as a control, or with 10 μM GA4 (T-Y), or 10 μM MeJA (Z-AE) without a MF (B, E, H, K, N, Q, T, W, Z, AC) or subjected

to a 500 mT MF (C-D, F-G, I-J, L-M, O-P, R-S, U-V, X-Y, AA-AB, AD-AE) under blue light (B-M, N-AE). Quantification of the primary root length of WT and *piezo-cl* mutant seedlings treated with ACC (AF-AG) ($WT_{1/2\ MS}$: n_{CK}=12, n_N=13, n_S=13; *piezo-cl*$_{1/2\ MS}$: n_{CK}=12, n_N=12, n_S=11; WT_{ACC}: n_{CK}=67, n_N=65, n_S=61; *piezo-cl*$_{ACC}$: n_{CK}=66, n_N=61, n_S=61), GA4 and MeJA (AH-AJ) (WT_{DMSO}: n_{CK}=23, n_N=30, n_S=23; *piezo-cl*$_{DMSO}$: n_{CK}=41, n_N=42, n_S=33; WT_{GA4}: n_{CK}=23, n_N=30, n_S=23; *piezo-cl*$_{GA4}$: n_{CK}=41, n_N=42, n_S=33; WT_{MeJA}: n_{CK}=23, n_N=30, n_S=23; *piezo-cl*$_{MeJA}$: n_{CK}=41, n_N=42, n_S=33). Arrows labeled "g" indicate the direction of gravity; the black, curved and solid lines with arrow heads represent the direction of the MF lines. The black dotted lines point to the N or S pole of the magnetic block, respectively. WT = wild-type. CK = seedlings not subjected to a MF, N = seedlings treated with the N pole of the magnetic block, S = seedlings treated with the S pole of the magnetic block. Blue = Seedlings treated with blue light. Data are means ±SE. ns = not significant, ** $P < 0.01$ (Student's *t*-test). Scale bar = 1 cm.

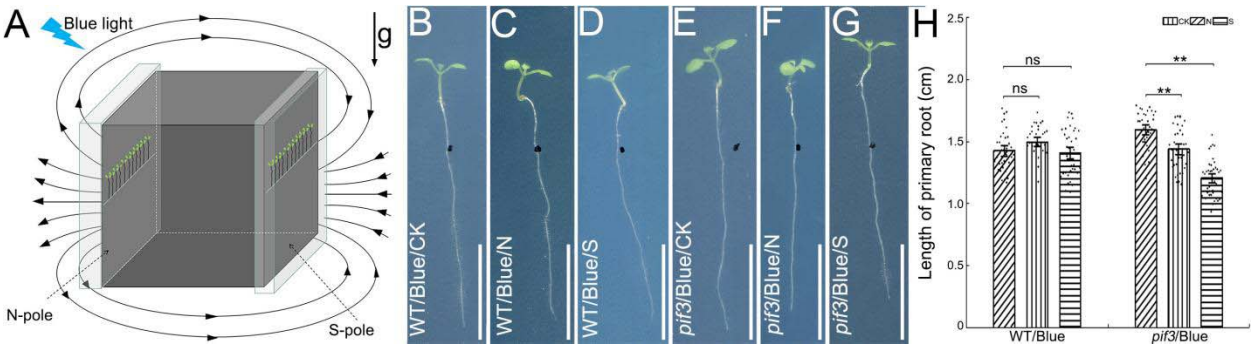

Fig. S10 Root phenotypes of *pif3* mutant seedlings subjected to a MF under blue light.

Schematic diagram of seedlings subjected to a MF under blue light (A). The root phenotypes of WT (B-D) and *pif3* mutant (E-G) seedlings not subjected to a MF (B, E), or subjected to a 500 mT MF (C-D, F-G) under blue light (B-G). Quantification of the primary root length of WT and *pif3* mutant (H) seedlings (WT: n_{CK}=35, n_N=33, n_S=38; *pif3*: n_{CK}=35, n_N=37, n_S=40). Arrows labeled "g" indicates the direction of gravity; the black, curved and solid lines with arrow heads represent the direction of the MF lines. The black dotted lines point to the N or S pole of the magnetic block, respectively. WT = wild-type. CK = seedlings not subjected to a MF, N = seedlings treated with the N pole of the magnetic block, S = seedlings treated with the S pole of the magnetic block. Blue = Seedlings treated with blue light. Data are means ± SE. ns = not significant, ** $P < 0.01$ (Student's *t*-test). Scale bar = 1 cm.

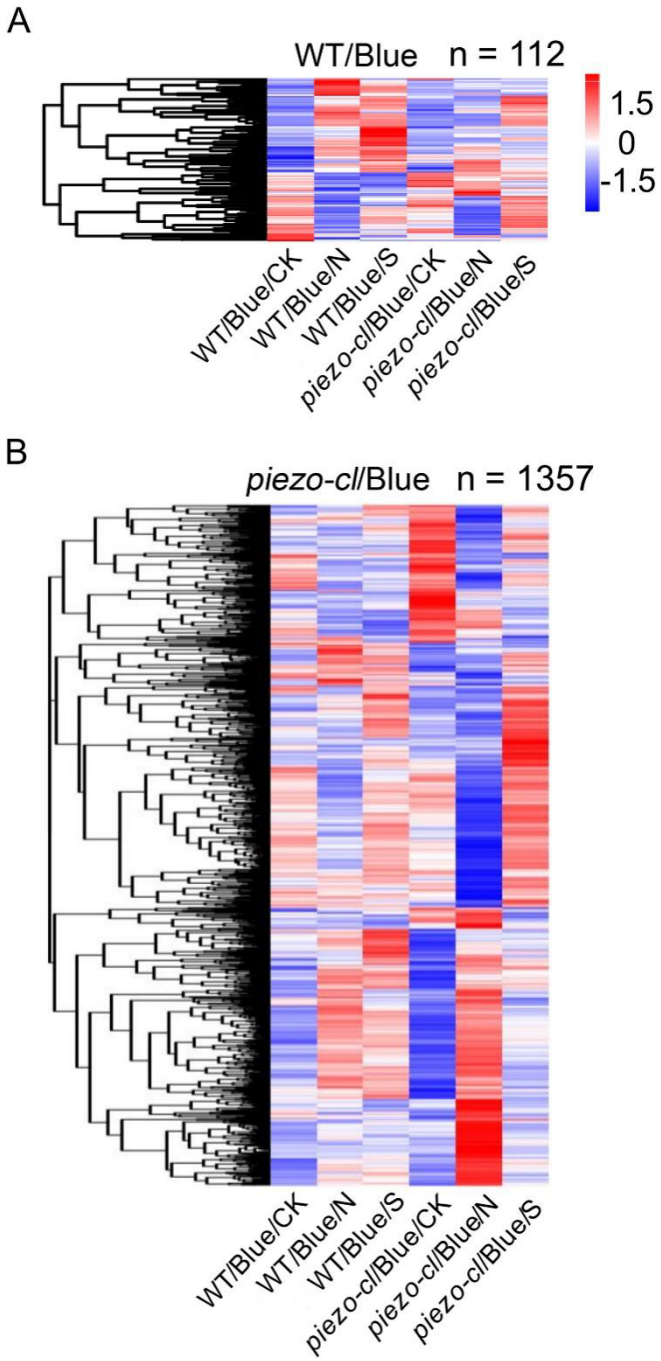

Fig.S11 Heatmap of *Arabidopsis* unigenes in WT and *piezo-cl* mutant seedlings subjected to a MF under blue light.

(A) Heatmap of DEGs in WT subjected to a MF under blue light, showing genes that exhibit either the same expression trend in response to both the N and S poles of the magnetic block or display specific changes in response to either the N or S pole of the magnetic block, compared to the control without MF treatment. (B) Heatmap of DEGs in *piezo-cl* seedlings subjected to a MF

under blue light, showing genes that exhibit either the same expression trend in response to both the N and S poles of the magnetic block or display specific changes in response to either the N or S pole of the magnetic block, compared to the control without MF treatment. Gene expression levels of RNA-seq are log10 transformed (normalized FPKM + 1). "n" represents the number of DEGs. WT = wild-type. CK = seedlings not subjected to a MF, N = seedlings treated with the N pole of the magnetic block, S = seedlings treated with the S pole of the magnetic block. Blue = Seedlings treated with blue light.

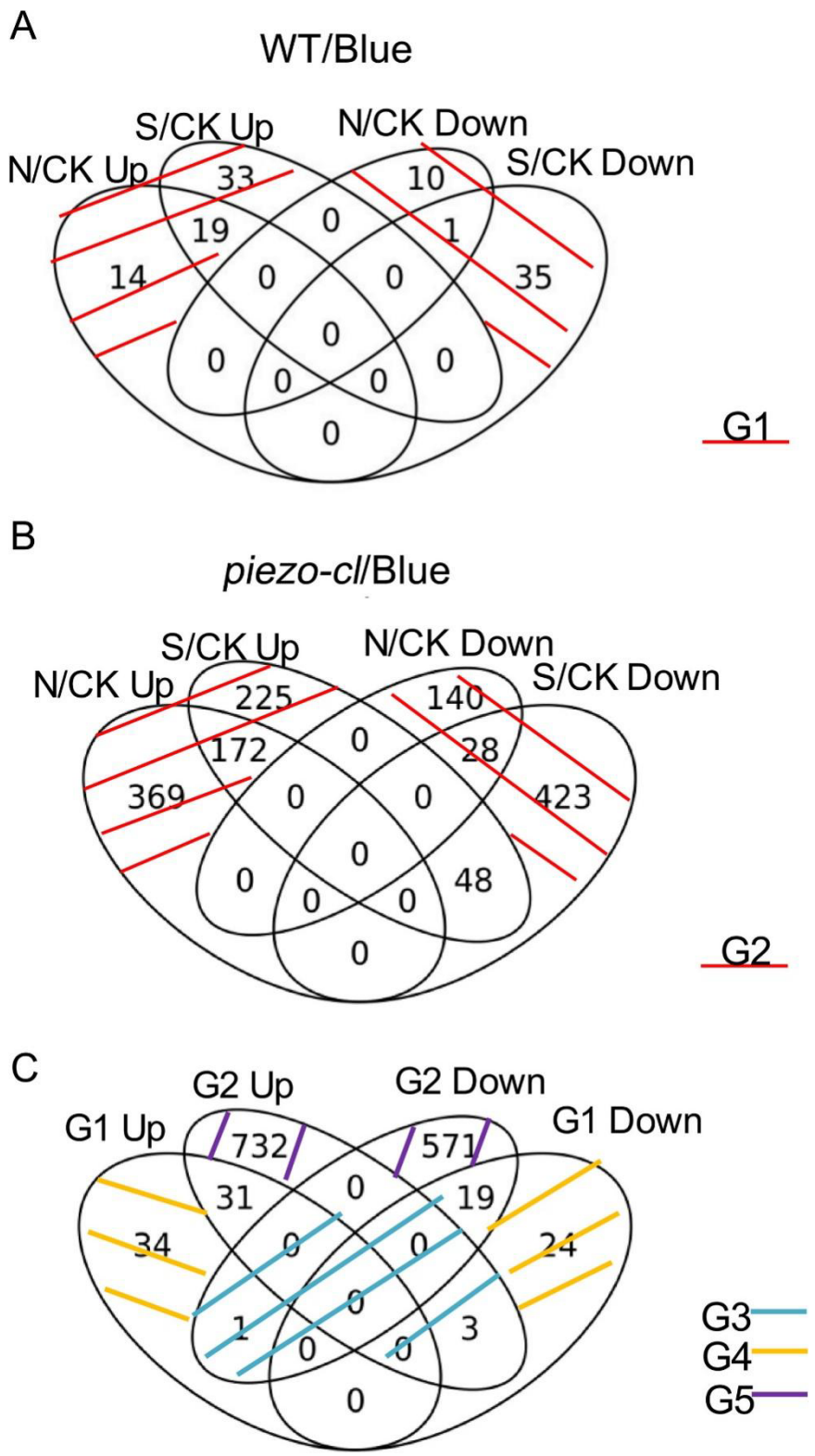

Fig.S12 Expression patterns of DEGs in *Arabidopsis* seedling root transcriptomes

DEGs in WT seedlings exhibit similar trends under both N and S poles of the magnetic block, as well as show specific changes under the N or S pole of the magnetic block under blue light (G1)

(A). DEGs in *piezo-cl* seedlings show consistent trends under both N and S poles of the magnetic block, with significant alterations specifically in response to either the N or S pole of the magnetic block under blue light (G2) (B). DEGs in seedlings grown in blue light that respond to MF regulation of root growth in both WT and *piezo-cl* mutant seedlings, but that exhibit different trends (G3), DEGs specifically responsive to MF treatment in WT seedlings (G4), and DEGs specifically responsive to MF treatment in *piezo-cl* mutant seedlings (G5) (C). WT = wild-type. CK = seedlings not subjected to a MF, N = seedlings treated with the N pole of the magnetic block, S = seedlings treated with the S pole of the magnetic block. Blue = Seedlings treated with blue light. up = up-regulated DEGs, down = down-regulated DEGs.

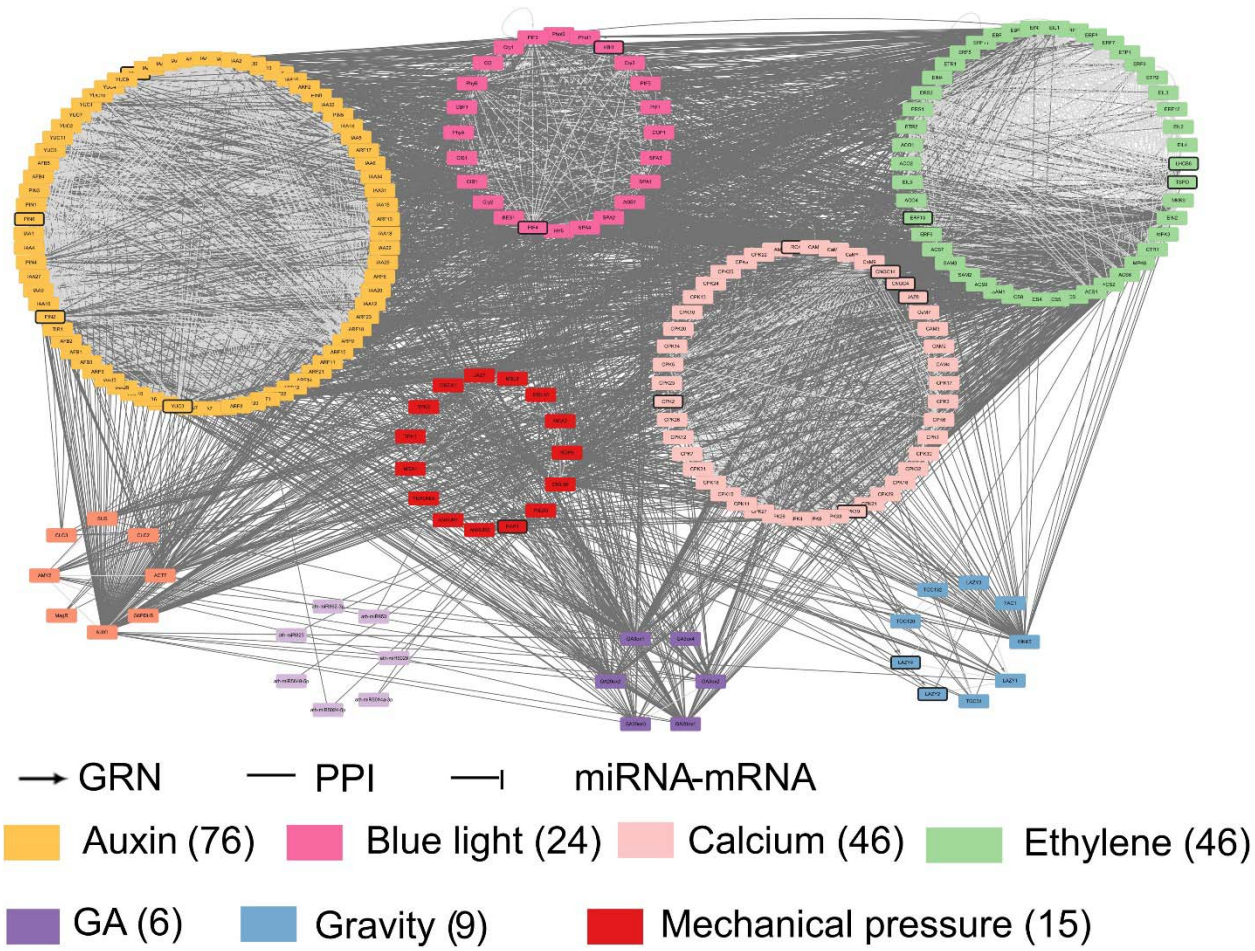

Fig.S13 Integrated gene regulatory network (iGRN) in the roots of WT and *piezo-cl* mutant seedlings subjected to MF under blue light.

The integrated network types include transcription factor regulatory networks (GRN), protein

interaction networks (PPI) and miRNA-targets regulatory networks (miRNA-mRNA). The numbers in parentheses represent the counts of different types of genes.

Table S2. Phytohormone- and light-related responsive elements in the *PIEZO* promoter

Name	Site	Strand	Organism	Sequences (5'-3')	Function
AE-box	1554	+	*Arabidopsis thaliana*	AGAAACTT	Part of a module for light response
G-box	515	-	*Arabidopsis thaliana*	TACGTG	Cis-acting regulatory element involved in light responsiveness
	1648	+	*Zea mays*	CACGAC	
P-box	1907	+	*Oryza sativa*	CCTTTTG	Gibberellin-responsive element
TATC-box	1966	-	*Oryza sativa*	TATCCCA	Cis-acting element involved in gibberellin-responsiveness
AuxRR-core	992	-	*Nicotiana tabacum*	GGTCCAT	Cis-acting regulatory element involved in auxin
I-box	1968	+	*Zea mays*	GGATAAGGTG	Part of a light responsive element
TCT-motif	645	-	*Arabidopsis thaliana*	TCTTAC	Part of a light responsive element
GT1-motif	1802	-	*Solanum tuberosum*	GTGTGTGAA'	Light responsive element
GA-motif	321	-	*Arabidopsis thaliana*	ATAGATAA	Part of a light responsive element
TCCC-motif	1123	-	*Spinacia oleracea*	TCTCCCT	Part of a light responsive element
	1374	-			
GATA-motif	913	+	*Solanum tuberosum*	AAGGATAAGG	Part of a light responsive element
CGTCA-motif	1415	+	*Hordeum vulgare*	CGTCA	Cis-acting regulatory element involved in the MeJA-responsiveness
GARE-motif	298	-	*Brassica oleracea*	TCTGTTG	Gibberellin-responsive element
	1299	-			

Table S3. Sequences of gene-specific primers for real-time PCR

Target gene	Primer	Sequence
AtActin2	Atactin2-FP	5’-TCCCTCAGCACATTCCAGCA-3’
	Atactin2-rP	5’-GATCCCATTCATAAAACCCCAGC-3’
AtPIEZO	Atpiezo-FP	5’-CCCCAAACGAGGCCTTAGTT-3’
	Atpiezo-RP	5’-ATGGCCTGGAGAGCTAGTGA-3’
AtGUS	AtGUSn2-FP	5’-GTACAGCGAAGAGGCAGTCAAC-3’
	AtGUSn2-RP	5’-GGTTCGTTGGCAATACTCCAC-3’
ath-miR5648-5p	AtmiR5648-loop-FP	5’-CGCGTTTGGAAATATTTGGC-3’
	AtmiR5648-loop-RP	5’-AGTGCAGGGTCCGAGGTATT-3’
AtPIN2	AtPIN2-FP	5’-CCTCGCCGCACTCTTTCTTTGG-3’
	AtPIN2-RP	5’-CCGTACATCGCCCTAAGCAATGG-3’
AtPIN6	AtPIN6-FP	5’-GTGCAAGATCTTCACGCCGG-3’
	AtPIN6-RP	5’-TGTCGGCGAGGATGAACATT-3’
AtRCA	AtRCA-FP	5’-GAACTCACCACGCTGTCCTT-3’
	AtRCA-RP	5’-CTTGACCTTTGCCTCCCCAT-3’
AtLHCB6	AtLHCB6-FP	5’-GCGATGGCAGCGGTTCTTG-3’
	AtLHCB6-RP	5’-CCATGGCGTTGCCCACTCA -3’
AtCPK2	AtCPK2-FP	5’-AGATGTGTGGAGTGCTGGTG-3’
	AtCPK2-RP	5’-CGCTTTCAGAGATGCTTGGC -3’
AtYUC5	AtYUC5-FP	5’-TTCAACGAGTGTGTCCAGTCTGCT-3’
	AtYUC5-RP	5’-TCTCTGGAACAACTTTCTCCGCGT -3’
AtCPK19	AtCPK19-FP	5’-GCGGCTCAAGTCCTAGAACA-3’
	AtCPK19-RP	5’-CATAGCTCGGAGTTGCTTCA-3’

AtCNGC4	AtCNGC4-FP	5’-GTCTCATGACTCTCAGCACA-3’
	AtCNGC4-RP	5’-GTAGCGTGCAGAAATACCTT-3’

References and Notes

C. Agliassa et al., Geomagnetic field impacts on cryptochrome and phytochrome signaling. *J Photochem Photobiol B* **185**. 32-40 (2018).

E. Bello-Bello and L. Herrera-Estrella. Breaking new ground: Decoding the root's molecular circuits to penetrate compacted soil. *Dev Cell* **59**, 431-433 (2024).

M. A. Ashraf. Evolutionarily conserved mechanosensor PIEZO in land plants. *Molecular Plant* **1**, 1782-1786 (2021).

M. Ahmad *et al*., Magnetic intensity affects cryptochrome-dependent responses in *Arabidopsis thaliana*. *Planta* **225**, 615-24 (2007).

M. Albaqami *et al*., Arabidopsis cryptochrome is responsive to Radiofrequency (RF) electromagnetic fields. *Sci Rep* **10**, 1126 (2020).

N. A. Belyavskaya. Biological effects due to weak magnetic field on plants. *Adv Space Res* **34**, 1566-74 (2004).

B. Coste *et al*., Piezo1 and Piezo2 are essential components of distinct mechanically activated cation channels. *Science* **330**, 55-60 (2010).

C. Chen et al., TBtools: An integrative toolkit developed for interactive analyses of big biological data. *Mol Plant* **13**. 1194-1202 (2020).

J. Chen et al., Amyloplast sedimentation repolarizes LAZYs to achieve gravity sensing in plants. *Cell* **186**:4788-4802 (2023).

M. J. Correll *et al*., Transcriptome analyses of *Arabidopsis thaliana* seedlings grown in space: implications for gravity-responsive genes. *Planta* **238**, 519-33 (2013).

R. C. Canamero *et al*., Cryptochrome photoreceptors cry1 and cry2 antagonistically regulate primary root elongation in *Arabidopsis thaliana*. *Planta* **224**, 995-1003 (2006).

S. Chakraborty *et al*., CYCLIC NUCLEOTIDE-GATED ION CHANNEL 2 modulates auxin homeostasis and signaling. *Plant Physiol* **187**, 1690-1703 (2021).

J. Feng et al., GFOLD: a generalized fold change for ranking differentially expressed genes from RNA-seq data. *Bioinformatics* **28**. 2782-8 (2012).

X. Fang *et al*., AtPiezo plays an important role in root cap mechanotransduction. *International Journal of Molecular Sciences* **22**, 467 (2021).

A. González-Vidal *et al*., Growth alteration of *Allium cepa* L. roots exposed to 1.5 mT, 25 Hz pulsed magnetic field. *Int J Environ Health Res* **32**, 2471-2483 (2022).

M. Grinberg *et al*., Effect of extremely low-frequency magnetic fields on light-induced electric reactions in wheat. *Plant Signal Behav* **17**, 2021664 (2022).

H. Hu. Zhang *et al*., Bioinformatics analysis for Piezo in rice. *Reproduction and Breeding* **1**, 108-113 (2021).

M. B. Hafeez *et al*., Growth, physiological, biochemical and molecular changes in plants induced by magnetic fields: A review. *Plant Biol (Stuttg)* **25**, 8-23 (2023).

L. Jiang et al., Salicylic acid inhibits rice endocytic protein trafficking mediated by OsPIN3t and clathrin to affect root growth. *Plant J* **115**. 155-174 (2023).

Y. Jin et al., Static magnetic field regulates Arabidopsis root growth via auxin signaling. *Sci Rep* **9**. 14384 (2019).

N. Leitão *et al*., Nuclear calcium signatures are associated with root development. *Nat Commun* **10**, 4865 (2019).

T. Li *et al*., Calcium signals are necessary to establish auxin transporter polarity in a plant stem cell niche. *Nat Commun* **10**, 726 (2019).

S. A. R. Mousavi *et al*., PIEZO ion channel is required for root mechanotransduction in *Arabidopsis thaliana*. *Proceedings of the National Academy of Sciences* **118**, e2102188118 (2021).

R. Narayana *et al*., Reduction of geomagnetic field (GMF) to near null magnetic field (NNMF) affects *Arabidopsis thaliana* root mineral nutrition. *Life Sci Space Res (Amst)* **19**, 43-50 (2018).

M. Pertea et al., Transcript-level expression analysis of RNA-seq experiments with HISAT, StringTie and Ballgown. *Nat Protoc* **11**. 1650–1667 (2016).

I. Radin *et al*., Plant PIEZO homologs modulate vacuole morphology during tip growth. *Science* **373**, 586-590 (2021).

B. Saletnik *et al*., The Static Magnetic Field Regulates the Structure, Biochemical Activity, and Gene Expression of Plants. *Molecules* **27**, 5823 (2022).

J. A. da Silva and J. Dobránszki. Magnetic fields: how is plant growth and development impacted?. *Protoplasma* **253**, 231-48 (2016).

F. Tapia-Belmonte *et al*., The Effects of Uniform and Nonuniform Magnetic Fields in Plant Growth: A Meta-Analysis Approach. *Bioelectromagnetics* **44**, 95-106 (2023).

A. Vashisth and D. K. Joshi, Growth characteristics of maize seeds exposed to magnetic field. *Bioelectromagnetics* **38**, 151-157 (2017).

S. Vanneste and J. Friml, Calcium: The Missing Link in Auxin Action. *Plants (Basel)* **2**, 650-75 (2013).

R. Wang *et al*., Auxin analog-induced Ca^{2+} signaling is independent of inhibition of endosomal aggregation in Arabidopsis roots. *J Exp Bot* **73**, 2308-2319 (2022).

C. Xu et al., Suppression of Arabidopsis flowering by near-null magnetic field is mediated by auxin. *Bioelectromagnetics* **39**. 15-24 (2018).

C. Xu *et al*., Suppression of Arabidopsis flowering by near-null magnetic field is affected by light. *Bioelectromagnetics* **36**, 476-479 (2015).

C. Xu et al., Gibberellins are involved in effect of near-null magnetic field on Arabidopsis flowering. *Bioelectromagnetics* **38**. 1-10 (2016).

F. Xu *et al*., The soil emergence-related transcription factor PIF3 controls root penetration by interacting with the receptor kinase FER. *Dev Cell* **59**, 434-447 (2024).

X. Yang *et al*., Structure deformation and curvature sensing of PIEZO1 in lipid membranes. *Nature* **604**, 377-383 (2022).

K. Zhang *et al*., Blue-light-induced PIN3 polarization for root negative phototropic response in Arabidopsiss. *Plant J* **76**, 308-21 (2013).

S. Zhai *et al*., PIN3-mediated auxin transport contributes to blue light-induced adventitious root formation in Arabidopsis. *Plant Sci* **312**, 111044 (2021).

S. Zhang *et al*., The calcium signaling module CaM-IQM destabilizes IAA-ARF interaction to regulate callus and lateral root formation. *Proc Natl Acad Sci U S A* **119**, e2202669119 (2022).

X. P. Zhang *et al*., Roles and mechanisms of Ca^{2+} in regulating primary root growth of plants. *Plant Signal Behav* **15**, 1748283 (2020).

Y. Zhao *et al*., Sensory circuitry controls cytosolic calcium-mediated phytochrome B phototransduction. *Cell* **186**, 1230-1243 (2023).

Acknowledgments:

We thank Professor Kai He (Lanzhou University) for her generous provision of the *piezo-cl* mutant and the transgenic *Arabidopsis* line expressing *ProPIEZO::GUS*. We also thank Professor Shuhua Yang (China Agricultural University) for the gift of the $cry_{1\text{-}104}$ and $cry_{2\text{-}1}$ mutant lines. Our thanks also go to Professor Haodong Chen (Tsinghua University) for provision of the *cry2/1* double mutant line.

Funding:

This work was supported by grants from the National Natural Science Foundation of China (Grant Nos. 32260085, 31860064), Central Guidance for Local Scientific and Technological Development Special Funds (202407AA110006). The Key Projects of Applied Basic Research Plan of Yunnan Province (Grant No. 202301AS070082), the Young and Middle-Aged Academic and Technical Leaders Reserve Talent Program in Yunnan Province (202205AC160076), the Young Talent Program of High-level Talent Plan in Yunnan Province (Grant No. YNQR-QNRC-2020-073) and Crop Varietal Improvement and Insect Pests Control by Nuclear Radiation.

Author contributions:

Y.D. initiated the project, Y.D. and C.L. supervised the project and designed the experiments; Z.P., W.Y. and M.D. performed the majority of the experiments and analyzed and prepared the figures; H.B., Y.L., N.P., Y.X. and L.G. performed additional experiments. Y.D., C.L., Z.P., W.Y., M.D. and H.B. analyzed the data. Y.D. and C.L. wrote and revised the paper with input from all authors.

Competing interests:

The authors declare no competing interests.

Data and materials availability:

All data are available in the manuscript or the supplementary materials. The raw data of transcriptomes have been uploaded to the Genome Sequence Archive (GSA) public database (https://ngdc.cncb.ac.cn/) under project number PRJCA027762.

SUPPLEMENTARY MATERIALS

Materials and Methods

Figs. S1 to S13

Tables S1 to S3

Materials and Methods

Plant materials and growth condition

The *Arabidopsis* lines used in this experiment were from an ecotype Columbia (WT) background, and included *piezo-c1* and *ProPIEZO::GUS* (Fang et al.,2021), *35S::PIEZO* lines, *piezo-T*, $cry_{1\text{-}104}$, $cry_{2\text{-}1}$, and *cry1/2* lines. The Arabidopsis *piezo-T* mutant line (NASCode:N663516) was purchased from AraShare (www.arashare.cn). *Arabidopsis* seeds were grown on 1/2 Murashige and Skoog (MS) medium (M5519; Sigma-Aldrich) containing 0.8 % agar and cold treated for 2 days in the dark at 4°C, and were then transferred to white light to grow 4 days at 22°C under 16 h light/8 h dark regime.

Four-day-old seedlings, where the primary root length was about 1 cm, were transferred to fresh 1/2 MS medium and tightly attached to the N and S poles on the surface of a NdFeB magnet N52 of strength 50, 200 or 500 mT (Hangzhou Permanent Magnet Group Co. Ltd, Hangzhou, China), in which the direction of the magnetic field (MF) was perpendicular to the direction of gravity. Seedlings were subjected to MF treatment under either red or blue light for 6

days. The blue light intensity was 96 μmol.m^{-2}.s^{-1} and red light intensity was 96 μmol.m^{-2}.s^{-1}. Primary root lengths were measured using the ImageJ 1.41 software.

To detect the effect of the direction of the MF on regulating root growth, seedlings in which the primary root length with about 1 cm were transferred to a new plate with 1/2 MS medium, and then the plate was placed on either the N pole or the S pole of a NdFeB magnet N52 of strength 500 mT, in which the direction of the MF was either antiparallel or parallel to the direction of gravity. Seedlings were grown under MF treatment for 6 days under red or blue light.

To check the effect of a MF on the medium, the plate containing 1/2 MS medium was attached to the N or S pole of a NdFeB magnet N52 of strength 500 mT for 6 days in the dark. Four-day-old *Arabidopsis* seedlings grown on 1/2 MS medium under white light, and in which the primary root length was about 1 cm, were transferred to the 1/2 MS medium pre-treated with a MF at strength 500 mT, and grown under blue light for 6 days.

Arabidopsis seedling root growth following treatment with auxin, GA, ethylene, MeJA and calcium ion inhibitor

Four-day-old seedlings in which the primary root length was about 1 cm were transferred to a plate containing 1/2 MS medium complemented with 5 μM of the auxin transport inhibitor TIBA, 0.01 μM NAA, 0.01 μM GA4, 100 μM ACC, 0.1 μM MeJA or 0.01 μM of the calcium ion inhibitor EGTA. The ACC and EGTA were dissolved in sterilized water. The chemicals TIBA, NAA, GA4 and MeJA were dissolved in DMSO, and seedlings treated with an equivalent volume of DMSO as a control. The plate containing the seedlings were attached to either the N or the S pole of a NdFeB magnet N52 of strength 500 mT and grown under blue light for 6 days.

Root growth of seedlings grown with the roots in darkness

To observe the effect of blue light on the expression of the *PIEZO* gene, transgenic seeds with *ProPIEZO::GUS* were grown in a plate containing 1/2 MS medium. A black baffle was placed below the seeds at a distance of 1cm, and with a tiny space between the surface of the medium and the baffle to ensure that the seedling roots were able to grow through the baffle. A piece of tinfoil was used to cover the plate above the baffle to produce a dark environment, where the roots did not receive any light. Additionally, a piece of tinfoil was also used to cover the area that

on the top of the seeds, so that light was prevented from directly irradiating into the space between the baffle and the medium, allowing the leaves to respond to light but keeping the roots in the dark. The seeds were sown on a plate with a baffle, tinfoil and the 1/2 MS medium, and were treated for 2 days at 4°C in darkness, and then the plates were transferred to blue light conditions and seedlings were grown for 4 days at 22°C. After 4 days, the plates together with the seedlings were transferred to a MF of strength 500 mT and grown for 6 days under blue light at 22°C.

GUS staining

Ten-day-old seedlings were collected and stained with GUS solution [50 mM $Na_2HPO_4 \cdot 12H_2O$, 50 mM $Na_2HPO_4 \cdot 2H_2O$, 10 % (v/v) Triton X-100, 2 mM $K_3[Fe(CN_6)]$, 2m M $K_4[Fe(CN_6)] \cdot 3H_20$, 10 mM EDTA, 1.04 mg/mL X-Gluc (R0851, Thermo Fisher Scientific)] at 37°C in darkness for 12 h. Then, The collected seedlings were then decolorized using ethanol. Samples were treated with ethanol at 30 %, 75 %, 90 %, and again 75 % (v/v) over 1 hour. Then, either the whole plant or just the root tip was observed and photographed using a Leica fluorescence microscope (DM2000, Leica, Germany).

Calcium ion flux measurement

Root caps of 6-day-old seedlings of wild-type and *piezo-c1* mutant lines were used to measure Ca^{2+} flux using Non-invasive Micro-test Technology (NMT). Firstly, 100 mM $CaCl_2$ filling solution was injected into the ion flow rate sensor (XY-CGQ-01) with a 4-5 μm aperture about 1.5cm long. Next, the Ca^{2+}-LIX exchanger (XY-SJ-Ca-10) was taken up by the tip of the LIX Holder (XY-LIX-01), and then the tip of Ca^{2+}-LIX exchanger was injected into the tip of the ion flow rate sensor with a syringe (XY-ZSQTZ-01) under the microscope. The Ca^{2+}-LIX exchanger at the tip of the holder was injected into the tip of the ion flow rate sensor using a syringe (XY-ZSQTZ-01) under the microscope. Then, a silver wire was chlorinated in silver chloride (XY-RY-05) for 25 seconds until it was an off-white color, and then inserted into the ion flux rate sensor, and the mounted ion flow rate sensor was connected to the pre-ion amplifier. The prepared Ca^{2+} flow rate sensors were also calibrated by the three-point calibration method using calibration solution 1, calibration solution 2 (XY-RY-02), and 0.1 mM $CaCl_2$ test solution (XY-

RY-01) with a theoretical value of 27 ± 5 mv/decade. The roots of seedling wild-type and *piezo-c1* lines were fixed to the bottom of a 35 mm petri dish (XY-PYM-35) using resin block (XY-SZK). 0.1 mM $CaCl_2$ (XY-RY-01) was added to submerge and stabilize the samples for 15 min, and then the samples were placed on the NMT microscope stage, the reference electrode (YG-CBDJ-01) was inserted into a 0.1 mM $CaCl_2$ solution (XY-RY-01), and the stage and preion amplifier were adjusted to position the Ca^{2+} flux rate sensor near the root cap of the primary root. Finally, the N or S pole of a magnetic rod of strength 120 mT was placed close to and above the root cap, and the blue filters of the NMT microscope were used as the blue light source. After root samples were stabilized in the test solution for 20 min, the Ca^{2+} flux was began to assay in a time course of 10 min for each data collection. Flow rate data were collected directly using the imFluxes V3.0 software (Xuyue.net) in picomole•cm^{-2}-s^{-1}, with positive values indicating Ca^{2+} efflux and negative values indicating Ca^{2+} influx. At least 7 roots were tested in each experiment for both the wild-type and *piezo-cl* mutant seedlings. All the reagents and consumable materials used in the experiments were purchased from Beijing Xuyue Technology Co. Ltd (Beijing, China).

RNA isolation and cDNA synthesis

The primary roots of 6-day-old wild-type or *piezo-c1* mutant seedlings that had been subjected to a 500 mT MF for 15 min, 30 min, 72 h or 144 h under blue light were collected. The primary roots of 6-day-old wild-type seedlings or seedlings expressing *ProPIEZO::GUS* subjected to 500 mT MF treatment for 6 days were used to isolate RNA. The isolation of RNA from the primary roots and cDNA biosynthesis referred to a previous report (Jiang et al., 2021).

Real-time PCR analysis

The relative quantitative gene expression levels were determined using an ABI QuantStudio 7 Flex Real-Time PCR System (Applied Biosystems, USA). The 10 μL PCR reaction mixture contained 5 μL NovoStart ® SYBR qPCR SuperMix Plus (Novoprotein Scientific lnc, Shanghai), 1 μL of cDNA template, 0.2 μL ROX2 (Novoprotein Scientific lnc, Shanghai), 3 μL RNase free H_2O and 0.8 μL of a 10 μM solution containing one of the following primer pairs: Atpiezo-FP and Atpiezo-RP, AtGUSn2-FP and AtGUSn2-RP, AtmiR5648-loop-FP and AtmiR5648-loop-RP, AtPIN2-FP and AtPIN2-RP, AtPIN6-FP and AtPIN6-RP, AtRCA-FP and AtRCA-RP,

AtLHCB6-FP and AtLHCB6-RP, AtCPK19-FP and AtCPK19-RP, AtYUC5-FP and AtYUC5-RP, AtCPK2-FP and AtCPK2-RP, or AtCGNC4-FP and AtCGNC4-RP, which were used to amplify the genes *AtPIEZO*, *GUS*, *ath-miR5648-5p*, *AtPIN2*, *AtPIN6*, *AtRCA*, *AtLHCB6*, *AtCPK19*, *AtYUC5*, *AtCPK2* and *AtCGNC4*, respectively (Supplemental Table S3). The *AtActin2* gene (AT3G18780) acted as the internal control, and was amplified with the primer pair AtActin2-FP and AtActin2-RP (Supplemental Table S3). PCR was performed under the following conditions: denaturation at 95°C for 2 minutes, followed by 40 cycles of 95°C for 45 seconds, 55-62°C for 30 seconds and 72°C for 1 minute. Three biological replicates were made. The relative gene expression levels were calculated by using the $2^{-\Delta\Delta Ct}$ method. The software SPSS version 19.0 (IBM, Inc., Armonk, NY, USA) was used to analyze differences in gene expression. * $P < 0.05$ was taken to indicate a statistical difference, ** $P < 0.01$ indicated a statistically significant difference.

Transcriptome analysis

Both of the raw RNA-seq and sRNA-seq reads were subjected to quality control with FastQC (v0.12.1). Subsequently, transcriptome analysis was performed using the HISAT2 pipeline (Pertea et al., 2016). The *Arabidopsis* genome version used was TAIR10, downloaded from the phytozome v13 (https://phytozome-next.jgi.doe.gov/). The differentially expressed genes were identified using GFOLD (Feng et al., 2012)

Construction of the integrated gene regulatory network

The integrated gene regulatory network encompasses three types of networks: the transcription factor regulatory network, with a score of more than 0.7 (Nature Plants 2021), the protein-protein interaction network (https://string-db.org/), with a score of more than 0.7 and the miRNA-target gene regulatory network. The regulation of target genes by miRNAs was predicted with psRNATarget (Nucleic Acids Research 2018). Sub-network was extracted with Ctyohubba tool and visualized in Cytoscape (v3.9.0).

Promoter analysis of *AtPIEZO* gene

The website Ensembl Plants website (http://plants.ensembl.org/index.html) was searched for the *AtPIEZO* (AT2G48060) sequence, and the 2000 bp upstream of the *AtPIEZO* gene was used to analyze the promoter structure using online software Plant Care (http://bioinformatics.psb.ugent.be/webtools/plantcare/html/). A visual representation was constructed using TBtools (Chen et al., 2020).

Statistical analysis

The ImageJ 1.41 software was used to measure root length, root growth angle and GUS level. All images were processed using the Photoshop software. Data were analyzed with one-way ANOVA or two-tailed Student's *t*-test, and the Origin 2022 and Photoshop were used to plot images.